Effect of recycled concrete aggregates and recycled filler on delayed ettringite formation: An experimental study compared to chemical modelling

Alexandre Yammine, Mahmoud Hamdadou, Nordine Leklou, François Bignonnet, Marta Choinska

Effect of recycled concrete aggregates and recycled filler on delayed ettringite formation : an experimental study compared to chemical modelling

Alexandre Yammine[a,*], Mahmoud Hamdadou[a], Nordine Leklou[a], François Bignonnet[a], & Marta Choinska-Colombel[a]
[a]Nantes Université, École Centrale Nantes, CNRS, GeM, UMR 6183, F-44600 Saint-Nazaire, France

Received Day Month Year; Accepted Day Month Year

Abstract

This study investigates the development of delayed ettringite formation in concrete made of recycled concrete aggregates (RCA) and in mortars with a recycled concrete filler. Experimental results are compared to a chemical model of delayed ettringite formation by Sellier & Multon (2018). Three concretes were formulated, one with natural siliceous aggregates and two others with two different RCA. Concrete and mortar samples were screened for one year for DEF damage. Results show that RCA based concrete did not develop DEF damage, but concrete made of siliceous aggregate did. Recycled filler had a small negative effect on DEF but not as much as limestone filler. Comparison to chemical modelling, including six additional mortars from Yammine (2020), shows that the produced expansive volume can not be directly linked to the measured expansion. The porosity of mortars and concrete plays an important role in controlling the expansion. All formulations that did exhibit large expansions had developed a maximum volume of expansive products higher than 30% of their porous volume. These results suggest a simple method to predict DEF related expansion in concrete with or without recycled concrete products.

Keywords: Delayed ettringite formation; concrete; chemical modelling; recycled aggregate; damage

1 Introduction

Concrete recycling is a major issue in the construction industry. The usage of recycled concrete aggregate (RCA) as a replacement of natural aggregate in concrete can be a viable and possible solution for limiting the environmental impact of quarry and the disposal of concrete waste [1, 2, 3, 4]. 1.7 tonnes of these RCA are produced per person per year in Europe, waiting to be valorized [5, 6]. Delayed ettringite formation (DEF) is a concrete damage related to an exposition to elevated temperature, particularly at an early age. Moreover, chemical composition is an important factor in DEF development [7, 8, 9]. Concrete made with RCA may be more prone to DEF as some of those aggregates are rich in DEF linked chemical compounds. Cement paste, a major component

*corresponding author: alexandre.yammine@univ-nantes.fr

of recycled concrete aggregates, is a source of ettringite, monosulphate, free sulphates and alkali. Additionally, pollution by different materials such as plaster, a sulphate rich material, is common in recycled aggregates [10]. As a consequence, the use of recycled concrete aggregates in concrete production is limited. The European standard EN 12620+A1 [11] sets an upper limit of 0.2% on RCA sulphate content. Some studies have shown that the use of recycled sand aggregates in mortars with higher sulphate content does not increase the possibility of delayed and secondary ettringite related expansion [12, 13, 14]. The French project RecyBéton [15] achieved similar results. These previous studies raise the question of the need to reassess the sulphate limit in standards, as the current limit is probably too strict.

Limits of the European standards on RCA usage in concrete may not be soon modified or removed. Consequently, one of the possible alternatives is to recycle concrete as a filler. This study evaluates the new and unknown impact of recycled filler on DEF. In addition, it will be interesting to confirm the experimental results using a simple predictive model of DEF expansion.

Thermodynamic and chemical mechanisms of DEF are complex phenomena that are still not completely understood, yet some thermodynamic and chemical models have shown their capacity to model DEF efficiently. Flatt and Scherer [16] proposed a thermodynamic model explaining the driving force of crystallization pressure. Salgues [17] developed a chemical model that predicts the kinetics and the amount of DEF based on the thermodynamic equilibrium with the interaction of alkaline sorption on C-S-H surface and aluminate fixation. Sellier & Multon [18] proposed a simple DEF chemical model able to predict expansion for several concrete formulations. The model includes alkali effect and aluminate fixation that can be applied easily. The chemical model must be coupled with a poro-mechanical model to simulate the expansion and its structural effects [18]. Yammine et al. proposed a poromechanical DEF damage model applied to mortars [19, 20]. The present article does not include the poro-mechanical part but only combines chemical modelling with experimental results to investigate in which conditions the expansive volume of DEF products can lead to expansions in RCA based concrete and mortars.

The objective of the current study are:

1. to further investigate the risk of DEF related expansion of concretes formulated with RCA through an experimental study

2. to investigate the risk DEF development of mortars including recycled concrete filler

3. to investigate the link between the expansive volume obtained from the chemical model of Sellier & Multon [18] and DEF related expansion in concrete and mortar formulations comprising recycled concrete aggregate or filler, which are extremely different from the formulations used to calibrate and validate that model.

The paper is organized as follows. The experimental study on concretes with RCA and mortars with recycled filler is presented in section 2. The chemical model of Sellier & Multon [18] and the identification of its input parameters for all concrete and mortars of our study is detailed in section 3. The link between the maximum modelled expansive volume and the maximum observed expansion is investigated in section 4, highlighting the existence of a threshold on the filling ratio of porosity by expansive products under which DEF related expansion is unlikely for investigated materials.

2 Experimental study

Five standardised mortars and three concretes are studied for delayed ettringite formation. All mortars are made of standard siliceous sand (§ 2.1.2), one without any addition, two with recycled filler (RF) and the remaining two with limestone filler (LF) (§ 2.1.5). Concrete formulations contain no addition apart from a plasticizer to enhance workability. One formulation made of natural siliceous aggregate (§ 2.1.3) and the two others made of 100% recycled concrete aggregate (RCA) including the recycled fine aggregate part (RFA) (§ 2.1.4). A cure phase composed of a four-stage heat treatment reaching 80°C is applied on all mortars and concrete.

2.1 Materials

2.1.1 Cements

Two CEM-I 52.5N CE CP2 NF cements are used in this study. Cement A is used only in mortar and Cement B only in concrete. Based on chemical and mineralogical characteristics in tab. 1, the two selected cements are rich in alkali, aluminates and sulphates, which increases concrete DEF likelihood when exposed to elevated temperature and humidity.

Table 1: Cements chemical composition.

Compound/property	Cement A	Cement B
Alkali equivalent Na_2O (% w/w)	0.8±0.05	0.77
SO_3 (% w/w)	3.1	3.71
Cl^- (% w/w)	0.04	0.07
S^{2-} (% w/w)	0.01	0.00
C_3S (% w/w)	63	54.1
C_2S (% w/w)	14	19.1
C_3A (% w/w)	9	9.9
C_4AF (% w/w)	9	9.7
Density (g/cm^3)	3.16	3.16
Blaine fineness (cm^2/g)	3829	4370
Loss on ignition (950°C) (% w/w)	1.2	1.18
Insoluble residue (% w/w)	0.3	0.27

2.1.2 CEN-standard sand

CEN-standard sand is used in all mortar formulations. Sand meets the standard NF EN 206+A1 [21] specification, it is classified as non-alkali silica reactive according to NF P18-594 [22].

2.1.3 Natural quartzite aggregates

Alkali-silica reaction proof quartzite aggregates are used in reference concrete (C-Ref). Concrete DEF reactivity made of these aggregates was confirmed in Amine et al. [23]. Moreover, alkali-silica reaction was not found in those concretes. Aggregates are provided in different sand and gravel grain sizes that correspond to concrete formulations

in § 2.2.1 which are [0/0.315], [0.315/1], [1/2] and [2/4] mm for sand and [4/8] and [8/12.5] mm for gravel.

2.1.4 Recycled concrete aggregates

Recycled concrete aggregates (RCA) have been ordered from two Construction & Demolition Waste platforms located near Paris and Quimper city in the west of France. The original grain size of aggregates was [0/20] mm. Several screening and sieving steps were done to meet the natural sand and gravel grain sizes in § 2.1.3. Sand was separated into [0/0.315], [0.315/1], [1/2] and [2/4] mm grain sizes and gravel into [4/8] and [8/12.5] grain sizes. [0/2] mm sand grain size of these RCA had been used to study DEF in recycled sand-based mortars by Yammine et al. [12].

RCA absorption and density : Absorption and density tests were done according to EN 1097-6 standard [24]. Results in tab. 2 show that Quimper RCA have higher absorption compared to that of Paris RCA, while the density is higher in Paris RCA. Higher absorption indicates higher porous volume which is mostly localized in the paste. Thus, considering same grain size, higher paste proportion is available in Quimper aggregate in comparison with Paris aggregate. As paste fraction increases, porous volume increases so density decreases.

Table 2: RCA absorption and density.

Grain size (mm)	Absorption (% w/w)		Density (g/cm^3)	
	Quimper	Paris	Quimper	Paris
[0/0.315]	16.0	12.0	-	-
[0.315/1]	14.9	7.7	-	-
[0/2]	14.5	10.0	1.9	2.1
[1/2]	9.0	5.9	-	-
[2/4]	8.5	5.5	2.12	-
[4/8]	7.3	5.3	2.21	2.3
[8/12.5]	5.5	4.9	2.25	-

RCA chemical characteristics : Soluble sulphate and water-soluble alkali content was determined according to NF EN 1744-1 [25] and LPC N°37 [26] standards respectively which are shown in tab. 3. In [0/2] mm sand, sulphate content in Quimper aggregate is 0.21 % and in Paris aggregate 0.29 %. Gravel has lower sulphate content due to its lower paste proportion compared to sand. The sulphate content of both RCA is not elevated, some studies found larger amounts of sulphates up to 1 % and even more [10]. The alkali content is quite different between the two RCA. Quimper have larger amounts of alkali, 1300 mg/kg in [0/2] mm sand, but only 686 mg/kg in Paris sand. Alkali content in gravel decreases for the same reasons as for sulphates due to lower paste proportion compared to sand. In Quimper RCA, specifically, the sand part is alkali rich which implies a higher possibility of DEF development than with Paris aggregate, this hypothesis was confirmed in mortars made of recycled sand in Yammine et al. [12].

Table 3: Soluble sulphate and water soluble alkali contents of RCA

Grain size (mm)	Quimper	Paris
	Soluble sulphates (SO_4^{2-} % w/w)	
[0/2]	0.21 ± 0,052	0.29 ± 0.052
[4/10]	0.14 ± 0,013	0.16 ± 0.010
[10/20]	0.11 ± 0,001	Unmeasured
	Alkali content (mg/kg eq.Na_2O)	
[0/2]	1300 ± 28	686 ± 11
[4/10]	700 ± 27	228 ± 2
[10/20]	561 ± 39	Unmeasured

2.1.5 Recycled and Limestone Filler

Recycled filler (RF) is obtained by crushing Quimper $8-20$ mm recycled aggregate and passing it through an 80 µm sieve. RF Blaine fineness was determined to be 7057 cm^2/g which is almost the double of cement A and B mentioned in tab. 1. Cement A, RF and LF (limestone filler) chemical composition are compared in tab. 4-5. RF is SiO_2 and Al_2O_3 rich, likewise as Yammine et al. found. Quimper RCA are rich in quartz and feldspar [12]. Quimper aggregate natural phase mineralogy reflects the geological nature of the French Brittany region from where it has been extracted. Measured RF alkali is **2.76 %**, which is largely greater than the amount in cement A of 0.8% and even greater than alkali content in [0-2] mm sand which is 1.3 % (tab. 3). Therefore crushing and sieving RCA has increased the alkali content and probably solubility in recycled filler.

Table 4: X-ray fluorescence analysis of cement A, recycled filler and limestone filler.

Compound	Cement A	Recycled filler	Limestone filler
SiO_2 (% w/w)	21.3	50.19	1.2
Al_2O_3 (% w/w)	5.51	10.22	/
Fe_2O_3 (% w/w)	2.96	2.5	/
CaO (% w/w)	65.39	16.83	97.5
MgO (% w/w)	1	0.79	/

Table 5: Chemical analysis of chloride, water-soluble sulphate, sulphide, water soluble alkali and density of cement A, recycled filler and limestone filler (NF EN 1744-1 [25] and LPC N°37 [26])

Compound	Cement A	Recycled filler	Limestone filler
SO_3 (% w/w)	3.1	0.86	0.01
Cl^- (% w/w)	0.04	/	0.0012
S^{2-} (% w/w)	0.01	/	0.0008
Na_2O eq. (% w/w)	0.8	2.76	0.005
Density (g/cm^3)	3.12	2.3	2.7

2.2 Preparation and conservation

2.2.1 Mortar and concrete formulations

Five standardised mortars each having different binder composition are formulated with the same amount of sodium sulphate to enhance DEF development (5% w/w total SO_3). Adding sodium sulphate is commonly used in DEF studies to amplify DEF effects [27, 12, 28, 29]. All formulations have a water-to-binder ratio = 0.5 and a sand-to-binder ratio = 3. Binder is 100 % cement A or blended with 10 % or 20 % of one of the fillers, RF or LF. Mortar formulations are detailed in tab. 6.

Three concretes having the same mass proportions of cement, water, sand and gravels are made, but each with a different aggregate. Concrete formulation presented in tab. 7 is taken from GranDuBé [30]. This study proposed an adequate concrete formulation applied to DEF related research. C-Ref is made of natural quartzite aggregate, C-Qpr of Quimper RCA and C-Prs of Paris RCA. A quantity of polycarboxylate superplasticizer is used in RCA concrete to enhance workability (see tab. 8). A lower concentration is used in C-Ref formulation while it is not needed for workability, only to reduce the difference of potential superplastizer impact on DEF between natural and recycled aggregates formulations.

Table 6: Mortar formulations

Mortar formulations	Cement A	RF	LF	Sand	Water	Na_2SO_4
M-Ref	450 g	-	-	1350 g	225 g	15.16
M-RF10	**405** g	**45** g	-	1350 g	225 g	15.16
M-RF20	**360** g	**90** g	-	1350 g	225 g	15.16
M-LF10	**405** g	-	**45** g	1350 g	225 g	15.16
M-LF20	**360** g	-	**90** g	1350 g	225 g	15.16

2.2.2 Mortar mixing procedure and casting

Mortar mixing and casting is done according to NF EN 196-1 standard [31]. Mortars are casted in prismatic stainless-steel moulds (ref. E0107; L0722-E0104/01) having dimensions of 40×40×160 mm^3. Three samples in each formulation were equipped with an upper and a lower stud to measure longitudinal expansion.

2.2.3 Concrete mixing procedure and casting

Cylindrical samples; H = 220 mm; D = 110 mm; are prepared of each formulation. RCA aggregates are prepared one day prior to mixing by adding the required water quantity for humidification according to the measurements in tab. 2, then mixing till obtaining a homogeneous color. Each humidified aggregate is kept in a closed plastic cylinder to be used in 24h [12].

Table 7: Concrete formulation excluding superplasticizer

Sand-to-cement ratio				gravel-to-cement ratio		Water-to-cement ratio
Sand grain sizes (mm)				Gravel grain sizes (mm)		Water
[0/0.315]	[0.315/1]	[1/4]	[2/4]	[4/8]	[8/12.5]	
98/424	180/424	189/424	202/424	195/424	907/424	201/424

Table 8: Superplasiticizer dosage

Concrete reference	Aggregate type	Superplasticizer-to-cement (w/w)
C-Ref	Natural quartzite aggregates	1.9 / 424
C-Qpr	Quimper RCA	3.0 / 424
C-Prs	Paris RCA	3.0 / 424

One mixing procedure is applied for recycled and natural aggregate concrete. Gravel, sand and cement are mixed together for one minute. Restart time counting, during the first 30 seconds water is added gradually with 2/3 the superplaticizer quantity. At 2 min 30 add the remaining superplaticizer. Continue mixing for 3 min 30. Tap water specification used in concrete mixing respects NF EN 1008 [32].

Concrete sampling, specimens and moulds requirements, casting and curing complies with NF EN 12350-1 [33], NF EN 12390-1 [34], NF EN 12390-2 [35] and FD P 18-457 [36] for all stages of concrete preparation.

Testing fresh concrete : slump test is done according NF EN 12350-2 [37] and concrete fresh density are measured. Results in fig. 1 show that RCA impacts concrete workability and density. C-Prs have the lowest workability and C-Qpr the lowest density which is coherent with the low Quimper RCA density compared to Paris RCA (see tab. 2).

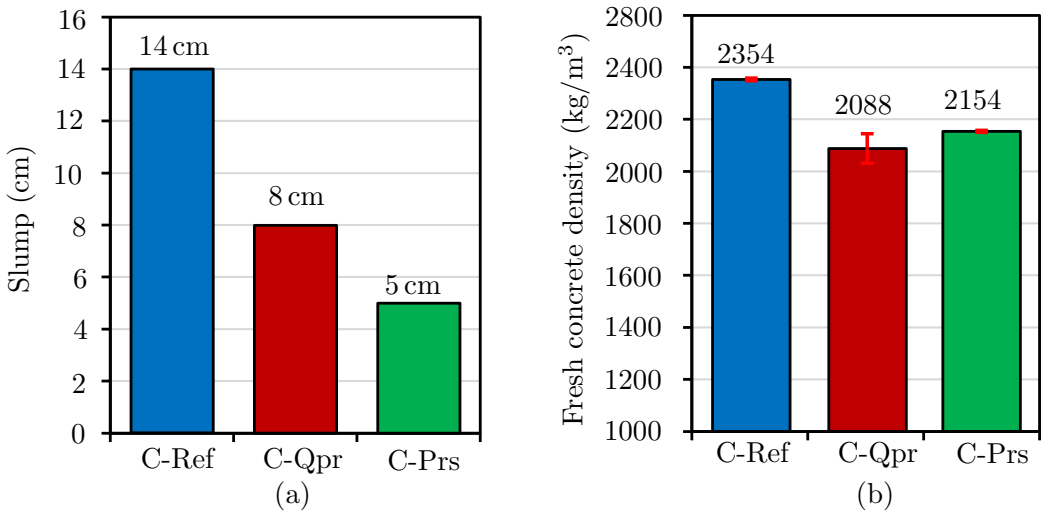

Figure 1: Slump and fresh concrete density. Density is measured on 3 samples for each concrete formulation.

2.2.4 Thermal curing and conservation

All casted moulds are covered by plastic films to protected them from drying during thermal curing. A four-stage thermal curing program is applied, as in Yammine et al. on mortars [12]. Temperature cycle starts at 20°C for 2 h, it increases linearly to 80 °C during 22 h (second stage) and stays at 80 °C for 72 h (third stage). Finally the temperature decreases linearly to 20 °C during 55 h (fourth stage). The temperature

was recorded using two thermocouples, one inserted in a mould and one placed in the oven.

When removed, mortars are stored in closed polypropylene plastic boxes filled with deionized water. Concrete cylinders are stored in big plastic containers filled with tap water. All mortar boxes and concrete containers are kept in a temperature controlled room at 20 °C. Enhancing alcali lixiviation and DEF development is done by renewing on a weekly and a monthly basis the water of mortar boxes and concrete containers respectively.

2.2.5 Samples monitoring and testing

Three mortar and concrete samples of each formulation were measured for expansion. An extensometer is used to measure mortar prisms expansion between the upper and the lower stud. On the other hand, each concrete cylinder is glued on it surface of revolution three steel pairs of balls to form between each an angle of 120°. The fixed three pairs balls are used for measuring the lengthening of the sample all around (see fig. 2). Sample expansion is computed as the mean of the three measured expansions.

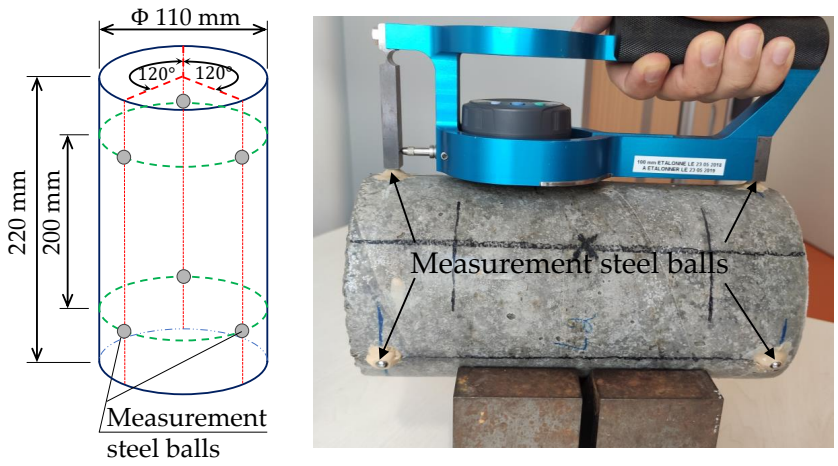

Figure 2: Diagram and photo of a concrete cylinder equipped with steel balls for elongation measurement.

Porosity and apparent density tests are done on concrete cylinders of 11 cm diameter and 5 cm height, and on 4 cm^3 cubes for mortars according to NF P 18-459 [38] standard. The test consists in measuring the buoyant mass of the saturated sample in water, the saturated surface-dry mass and the oven-dry mass at 105 °C. Three samples are tested on each measurement to determine porosity mean value and the corresponding standard deviation.

2.3 Experimental results

Expansion is a widely studied indicator in sulphate attack, whether internal or external, as it is a simple, repeatable and precise measurement. Expansion was monitored over 14 months on concrete and 7 months on mortars. Fig. 3 shows that mortars reached 0.04 % expansion at 30 - 35 days of conservation in water. The 0.04 % expansion value is considered a positive indicator for DEF damage according to LCPC [39]. Mortar

expansion increased considerably between 30 and 120 days, 0.50 % for M-Ref and M-RF10, 0.44 % for M-RF20, 0.40 % for M-LF10, and the lowest was 0.12 % for M-LF20. Expansion of mortars continued growing very slowly after 120 days. However for concretes, expansion exceeded the DEF indicator limit only for C-Ref. Expansion reached 0.04 % at 45 days for C-Ref and kept increasing to a maximum of 0.18 %, but reached 0.03 % for C-Qpr and 0.02 % for C-Prs at 45 days and then stopped increasing. Recall mortars are formulated with additional sodium sulphate to enhance DEF, while not concretes.

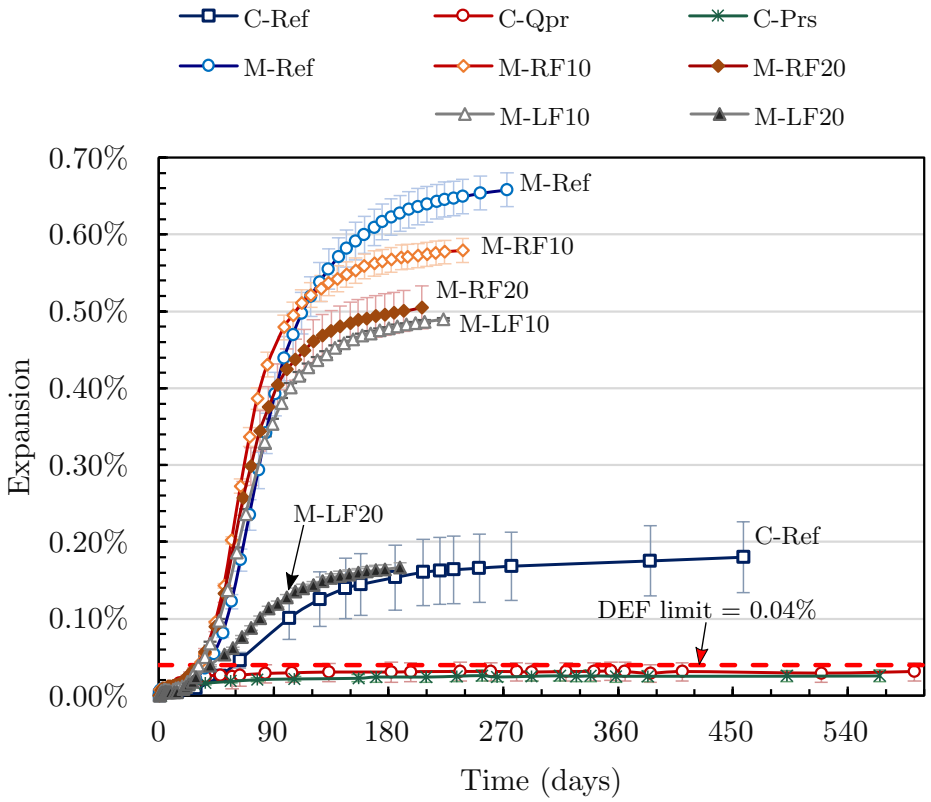

Figure 3: Concrete and mortar axial expansion. The height of error bars is twice the expansion standard deviation of three samples.

2.3.1 Effect of fine recycled particles in mortars

According to fig. 3 all mortars seem to behave almost similarly, as they have close expansion time characteristics. Expansion starts and slows in the same time interval which means that the characteristics of diffusion, sulphate desorption, alkali lixiviation are relatively close between all mortars. Expansion is slightly faster in recycled filler mortars than the reference mortar (M-Ref), and to a lesser extent in M-LF10 but not in M-LF20 due to limestone inhibiting impact on DEF, as explained at the end of this paragraph. At 6 months, M-Ref had the highest expansion about 0.64 %, M-RF10; 0.58 %, M-RF20; 0.5 %, M-LF10; 0.48 % and the lowest M-LF20 had 0.16 %. Recycled aggregate filler (RF) had a inhibiting impact on DEF expansion, this could be explained by the lower sulphate concentration in RF compared to cement A, 0.86 % v.s. 3.1 % (see tab. 5), however higher alkali concentration is found in RF (2.76 % in RF v.s.

0.8 % in Cem. A). Limestone filler shows more inhibiting impact on DEF expansion as a consequence of aluminates consumption by calcium carbonate [28]. This reaction produces monocarboaluminates [40, 41] and diminishes available aluminates quantities for ettringite formation.

Mortar porosity on 28, 90 and 180 days is shown in fig. 4. At 28 days, reference mortar and both mortars with 10 % filler had 16,5 % porosity versus 18 % for both mortars with 20 % filler. At 90 and 180 days, M-Ref, M-RF10 and M-RF20 had gradual increase of their porosity, while for M-LF10 it increased in the 28 - 90 days investigation period and decreased lightly in the 90 - 180 period, but was still higher than at 28 days. The evolution of porosity in mortars that undergo DEF is difficult to interpret due to the competition of two mechanisms [42, 43]: on the one hand, ettringite fills partially some pores, which tends to decrease porosity ; on the other hand, expansion is associated to microcracking, which tends to increase porosity. Additionally, Yammine et al. [12] found increasing porosity in heat cured mortars without expansion in recycled sand mortars and justify it by the unsuitability of the porosity test to measure accurately the porosity of highly porous material as recycled sand based mortars.

Recycled and limestone fillers at 10 % replacement in cement exhibit similar porosity at 28 days comparing to M-Ref, while at 20 % their porosity is 1.5 % greater than M-Ref. At 180 days, M-Ref porosity increased more than for other mortars and reaches equal porosity as the RF-mortars and higher porosity than the LF-mortars. Limestone filler may have played a role in lessening porosity growth which could be the results of new phases produced from limestone reaction with some cement phases [44, 40].

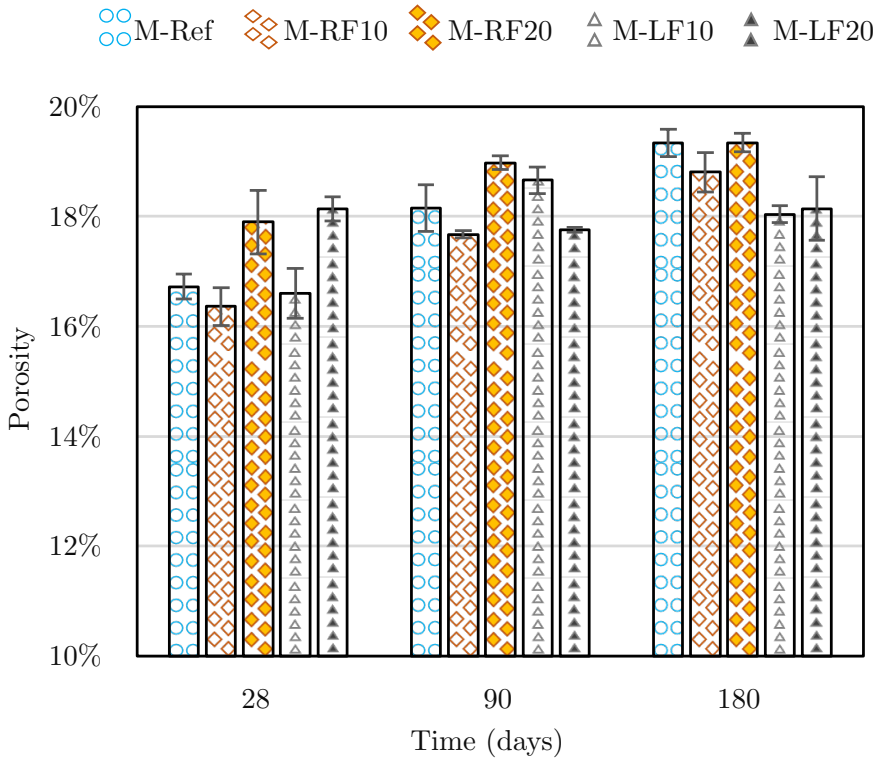

Figure 4: Mortar porosity at 28, 90 and 180 days after immersion in water

2.3.2 Effect of RCA in concrete

Natural aggregate concrete exhibited DEF expansion (fig. 3) reaching 0.18 % in a year of conservation in water but recycled aggregate concrete (C-Qpr and C-Prs) had an expansion below 0.04 %. This result is to be aligned with the results obtained on recycled sand based mortars by Yammine et al. [12] and Colman et al. [13, 14] that exhibited a low DEF expansion. The high porosity of recycled sand mortars has been proposed to be the primary factor in the reduction or cancellation of swelling by DEF, as the volume of delayed ettringite can easily crystallise at low pressure [45, 16, 14].

Concrete porosity and apparent density are graphically illustrated in fig. 5. C-Ref had the lowest porosity: starting from 15.5 % at 28 days it decreased with time to 14.2 % at 6 months and 13.9 % after one year. The decrease in porosity is likely related to the hydration of remaining anhydrous cement and to a lesser extent to filling some pores by non expansive delayed ettringite as some studies have proposed [42, 43]. Recycled aggregate concrete had higher porosity than C-Ref which is an expected result. C-Qpr had the highest porosity, starting from 25.2 % at 28 days while C-Prs had 22.1 % at the same age. Porosity of recycled aggregate concrete increased with time, mostly between 28 and 90 days. It remained almost stable after 90 days. Increasing porosity was remarked in recycled sand mortars [12]. As for RCA based mortars, we believe that the high porosity of RCA based concretes lead to a partial saturation of the samples after immersion in water for 48h in the porosity measurement procedure (§ 2.2.5), which caused biased porosity results (particularly at the age of first measure after heat cure).

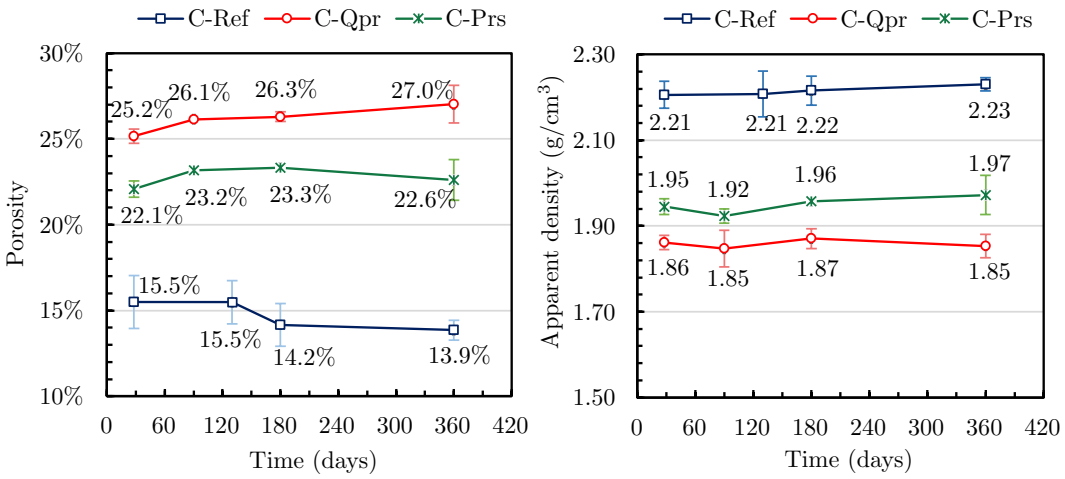

Figure 5: Porosity and apparent density of concrete at 28, 90, 180 and 360 days after immersion in water

3 Modelling delayed ettringite formation using Sellier & Multon chemical model

Sellier & Multon [18] model is able to determine the macroscopic evolution of the number of moles per unit volume of concrete of primary ettringite noted E_1, delayed

$$\text{If } \frac{S_c}{A_c} > 3 \begin{cases} E_1 = A_c \\ M_1 = 0 \\ \widetilde{A} = 0 \\ \widetilde{S} = S_c - E_1 \\ G = 0 \\ E_2 = 0 \end{cases} \qquad \text{If } 1 \leq \frac{S_c}{A_c} \leq 3 \begin{cases} E_1 = \dfrac{S_c - A_c}{2} \\ M_1 = \dfrac{3A_c^2 - S_c}{2} \\ \widetilde{A} = 0 \\ \widetilde{S} = 0 \\ G = 0 \\ E_2 = 0 \end{cases} \qquad \text{If } \frac{S_c}{A_c} < 1 \begin{cases} E_1 = 0 \\ M_1 = S_c \\ \widetilde{A} = A_c - M_1 \\ \widetilde{S} = 0 \\ G = 0 \\ E_2 = 0 \end{cases}$$

Table 9: The three different initial stoichiometric balance states corresponding to complete hydration reactions.

ettringite noted E_2, free sulphates ($\tilde{S}$), free aluminates ($\tilde{A}$), monosulphate (M_1) and hydrogarnet (G) or carboaluminate quantities in the case of limestone aggregates. In the latter case, it is most likely that the characteristic precipitation time is different from that of hydrogarnet since the addition of limestone filler has been shown to inhibit DEF [23].

3.1 Model initial conditions

Total sulphates content and aluminates content noted respectively S_c and A_c are constant and equal to :

$$A_c = E_1 + E_2 + M_1 + G + \tilde{A} \tag{1}$$
$$S_c = 3(E_1 + E_2) + M_1 + \tilde{S} \tag{2}$$

The initial conditions of the state variables A_c and S_c are given by :

$$A_c = \mathrm{C_3A^{eq}} = \mathrm{C_3A} + 2\,\mathrm{C_4AF} = \mathrm{A} + \mathrm{F} \tag{3}$$
$$S_c = \mathrm{C\overline{S}} + \mathrm{Na\overline{S}} \tag{4}$$

Aluminates and ferrites are merged together in an equivalent mole number noted $\mathrm{C_3A^{eq}}$ in eq. (3). Ferrites are considered able to replace aluminates and to produce ferrite rich ettringite, but they may modify the kinetics, mostly at the end of DEF. Initial sulphates content S_c is equal to the sulphates of gypsum in the cement and of sodium sulphate addition that is added in mortars formulations (§ 2.2.1). Sulphates are adsorbed on C-S-H and are exchanged with the porous solution to reach an equilibrium which is influenced by alkali concentration and temperature [46]. Ferrite ratio and sulphates adsorption impact DEF but are not taken in the model due to lack of sufficient experimental results according to authors.

Three initial different states can be defined using the stoichiometry balance of complete hydration reactions. Initial content of the six modelled species are defined in tab. 9.

3.2 Model principles and reactions

Three reactions are modelled: first sulfoaluminates dissolution, second free aluminates fixation into hydrogarnet and third sulphate and aluminates precipitation into delayed ettringite and/or conversion of available monosulphate and free sulphates into secondary/delayed ettringite. $T_{\mathrm{th,d}}$ and $T_{\mathrm{th,f}}$ are the minimum threshold temperatures for

dissolution and fixation respectively.

(R1) When $T > T_{\text{th,d}}$, the following differential equations describe the rate of sulfoaluminate formation or consumption with τ_d the characteristic time of dissolution:

$$\begin{cases} \dfrac{\partial E_1}{\partial t} = -\dfrac{E_1}{\tau_d} \\ \dfrac{\partial M_1}{\partial t} = -\dfrac{M_1}{\tau_d} \\ \dfrac{\partial E_2}{\partial t} = -\dfrac{E_2}{\tau_d} \end{cases} \tag{5}$$

(R2) When $T > T_{\text{th,f}}$, fixation starts consuming aluminates with a characteristic time τ_f. $T_{\text{th,d}}$ and $T_{\text{th,f}}$ are relatively close so fixation and dissolution are quasi-simultaneous reactions. The formation/consumption rates of free sulphates and aluminates are determined using the stoichiometric factors of dissolution and fixation:

$$\frac{\partial \tilde{S}}{\partial t} = -3\left(\frac{\partial E_1}{\partial t} + \frac{\partial E_2}{\partial t}\right) - \left(\frac{\partial M_1}{\partial t}\right) \tag{6}$$

$$\frac{\partial \tilde{A}}{\partial t} = -\left(\frac{\partial E_1}{\partial t} + \frac{\partial E_2}{\partial t} + \frac{\partial M_1}{\partial t}\right) - \frac{\tilde{A}}{\tau_f} \tag{7}$$

(R3) When $T < T_{\text{th,d}}$, precipitation produces delayed ettringite and consumes free species. The rate of delayed ettringite formation is controlled by the amount of free sulphates and the characteristic time of precipitation:

$$\frac{\partial E_2}{\partial t} = \frac{\tilde{S}}{\tau_p} \tag{8}$$

In some cases monosulphate subsists after a hot curing period ; it then combines during precipitation phase with free sulphates to form delayed ettringite. In this case the following equations applies:

$$\text{If } M_1 > 0 \begin{cases} \dfrac{\partial M_1}{\partial t} = -\dfrac{\partial E_2}{\partial t} \\ \dfrac{\partial \tilde{S}}{\partial t} = -2\dfrac{\partial E_2}{\partial t} \\ \dfrac{\partial \tilde{A}}{\partial t} = 0 \end{cases} \tag{9}$$

If all monosulphate has been consumed by eq. (9) or dissolved by eq. (6) then the DEF continues as follows till the complete consumption of the limiting reagent:

Table 10: Temperature and alkali concentration activation coefficients C_R^F according to Sellier & Multon [18].

R: reaction	F: activating factor	
	Temperature (T)	Alkali concentration (C)
Dissolution (d)	$\exp\left(-\frac{\mathrm{Ea}_d}{R}\left(\frac{1}{T}-\frac{1}{T_{th,d}}\right)\right)-1\geq 0$	$\frac{[\mathrm{Na}]}{[\mathrm{Na}_k]}$
Fixation (f)	$\exp\left(-\frac{\mathrm{Ea}_f}{R}\left(\frac{1}{T}-\frac{1}{T_{th,f}}\right)\right)-1\geq 0$	$\left(\frac{[\mathrm{Na}_k]}{[\mathrm{Na}]}\right)^m$
Precipitation (p)	$\exp\left(-\frac{\mathrm{Ea}_p}{R}\left(\frac{1}{T}-\frac{1}{T_p^{ref}}\right)\right)\frac{C_d^T(T)}{C_d^T(T_p^{ref})}$	$\begin{cases}\left(1-\frac{[\mathrm{Na}]}{[\mathrm{Na}]^{bl}}\right)^m, \text{ if } [\mathrm{Na}]<[\mathrm{Na}^{bl}]\\ 0, \text{ if } [\mathrm{Na}]>[\mathrm{Na}^{bl}]\end{cases}$

$$\text{If } M_1 = 0 \begin{cases} \dfrac{\partial M_1}{\partial t} = 0 \\ \dfrac{\partial \tilde{S}}{\partial t} = -3\dfrac{\partial E_2}{\partial t} \\ \dfrac{\partial \tilde{A}}{\partial t} = -\dfrac{\partial E_2}{\partial t} \end{cases} \tag{10}$$

3.3 Model parameters

Three parameters impact the three reactions (R1); (R2) and (R3):

1. Alkali concentration, denoted [Na], is the sum of the molar concentrations of sodium and potassium ions in pore solution. It impacts the temperature threshold of dissolution and the kinetics of dissolution and precipitation of ettringite.

2. Temperature (T) activates chemical reactions.

3. Water partial saturation of concrete or mortar porosity limits the kinetics of DEF precipitation. In the case of our experiments described in section 2, all samples are considered fully saturated as they are kept immersed in water. The influence parameters related to saturation are hence considered equal to one.

Characteristic times are defined as functions of reference characteristic times (τ_d^{ref}; τ_f^{ref}; τ_p^{ref}) and three activating coefficients each dependent of one of the three parameters (T, H, C):

$$\begin{cases} \frac{1}{\tau_d} = \frac{1}{\tau_d^{\mathrm{ref}}} C_d^T C_d^H C_d^C \\ \frac{1}{\tau_f} = \frac{1}{\tau_f^{\mathrm{ref}}} C_f^T C_f^H C_f^C \\ \frac{1}{\tau_p} = \frac{1}{\tau_p^{\mathrm{ref}}} C_p^T C_p^H C_p^C \end{cases} \tag{11}$$

Activation coefficients are noted C_R^F. F specifies the activating factor, noted T for temperature, H for saturation and C for alkali concentration. R specifies the impacted reaction noted d for dissolution, f for fixation and p for precipitation. Thus C_d^T is the temperature coefficient modulating dissolution kinetic. Saturation activation coefficients are considered in this study $C^H = 1$ as all samples have been stored in water. C^T and C^C equations are given in tab. 10. Reference characteristic times and parameters of the activation coefficients are given in tab. 11.

The dissolution threshold temperature $T_{th,d}$ is affected by alkali concentration; T_0 equals to 273.15 K:

$$T_{th,d} = T_0 + \begin{cases} T_{th,ref} & \text{, if } [\text{Na}] < [\text{Na}_k] \\ T_{th,ref} \left(\dfrac{[\text{Na}_k]}{[\text{Na}]} \right)^n & \text{, if } [\text{Na}] \geq [\text{Na}_k] \end{cases} \tag{12}$$

Table 11 defines and gives the values of all the parameters used in the model.

Table 11: Model parameters values according to Sellier & Multon [18].

Parameter	definition	Value	Unit
$T_{th,ref}$	Dissolution temperature at $[\text{Na}_k]$	80	°C
$T_{th,f}$	Threshold temperature for the fixation of aluminates	70	°C
T_p^{ref}	Reference temperature used to determine τ_p	20	°C
$[\text{Na}_k]$	Characteristic alkali concentration related to dissolution	0.28	mol.l^{-1}
$[\text{Na}]^{bl}$	Alkali concentration above which the DEF is impeded	0.96	mol.l^{-1}
n	Exponent for low dissolution temperature when $[\text{Na}] \geq [\text{Na}_k]$	0.18	–
m	Exponent for reducing aluminates fixation at high alkali	3	–
$\tau_d^{\text{ref}(1)}$	Sulfoaluminates dissolution characteristic time	65	hours
$\tau_p^{\text{ref}(1)}$	Ettringite precipitation characteristic time	30	days
$\tau_f^{\text{ref}(1)}$	Aluminates fixation characteristic time	30	hours
Ea_d	Energy activation for the dissolution	80	kJ.mol^{-1}
Ea_f	Energy activation for aluminates fixation	180	kJ.mol^{-1}
Ea_p	Energy activation for precipitation/DEF	44	kJ.mol^{-1}

(1) corresponding for C^{T}, C^{H} et C^{C} equal to 1.

3.4 Reagents content estimation

Reagents content is estimated using chemical characteristics and proportions of all constituents in concrete and mortar formulations. Pore volume is considered fully saturated. sulphates and aluminates content are defined as the molar number of each specie in a unit volume of material. Alkali content is defined as the molar number of alkali ions in a unit volume of pore solution. Tables 12; 13; 14 show aluminates, sulphates and alkali contents of the three concrete formulations C-Ref, C-Qpr and C-Prs and the three mortar formulations M-Ref, M-RF10 and M-RF20. Mortars from Yammine et al. [12] (Ref, Ref-SS, Qpr, Qpr-SS, Prs and Prs-SS) are added to the study. Concrete porosity values corresponds to porosity measurement at 28 days already shown in fig. 5. Mortar porosity is set to 18 % for all formulations. Effective cement content decreases when replacing natural aggregates by RCA. As formulation proportions are based on weight ratios, RCA volume will be higher in comparison with natural aggregates in a unit volume of mortar or concrete. Percentages of Al_2O_3, Fe_2O_3, Na_2O and SO_3 content in tab. 12-14 are mass fraction in cement and not in concrete. A_c and S_c are molar amounts of aluminates and sulphates in one m^3 of concrete or mortar including content of RCA, recycled filler and sodium sulphate if added.

RCA composition in tab. 13 is determined using chemical (tab. 3) and X-ray diffraction analysis. Total sulphates content was obtained with X-ray diffraction. $[\text{Na}_0]$ is initial alkali concentration including alkali from RCA. When sodium sulphate is used, two cases of alkali concentration are considered (see tab. 14):

- Case N°1: alkali content is drawn from cement and RCA only ;
- Case N°2: alkali content is drawn from cement, RCA and added sodium sulphate.

Ratios S_c/A_c are less than 1, which indicates according to tab. 9 that initial composition of cement paste before heat curing will be free from primary ettringite and only monosulphate will be available for dissolution with excess aluminates. Aluminates measurement using X-ray diffraction is more complex than sulphate for the reason that RCA are feldspar rich, meaning that the major amount of measured aluminates will not be of the form of monosulphate. A solution for that is to take the upper and lower limits for aluminates content in RCA and to determine the upper and lower limits of S_c/A_c. In the case where S_c/A_c is always < 3, then sulphates content determines delayed ettringite formation quantity. The given content of Al_2O_3 in RCA in tab. 13 is the maximum limit which corresponds to the case where sulphates and aluminates have equal molar number. In that case all sulfoaluminates are found in the form of monosulphate. The lowest content of aluminates is found when all sulfoaluminates are in the form of ettringite. In the latter aluminate molar quantity is the third of sulphates. After computing the lowest limit of aluminates content in RCA, the A_c/S_c is still < 1. Thus, it is not important to determine A_c exactly. For the sake of simplicity, aluminates molar content in RCA and in recycled filler is taken equal to that of sulphates.

Table 12: Estimation of sulphates, aluminates and alkali in concrete formulations.

Form.	ϕ (%)	Cement$^{(1)}$ (kg/m^3)	$Al_2O_3{}^{(2)}$ (%)	$Fe_2O_3{}^{(2)}$ (%)	$Na_2O^{(2)}$ (%)	$SO_3{}^{(2)}$ (%)	$A_c^{(3)}$ (mol/m^3)	$S_c^{(3)}$ (mol/m^3)	S_c/A_c -	$[Na_0]$ (mol.l^{-1})
C-Ref	15.5%	416.2	5.77%	3.19%	0.8%	3.7%	319	193	0,61	0,677
C-Qpr	25.2%	354.9	5.77%	3.19%	0.8%	3.7%	339	257	0,76	0,526
C-Prs	22.1%	376.2	5.77%	3.19%	0.8%	3.7%	347	268	0,77	0,515

(1) Effective cement content different than cement content in tab.7.
(2) Content in cement only.
(3) Including amounts from GBR if applicable, see tab. 13.

Table 13: Estimation of sulphates, aluminates and alkali in RCA for C-Qpr and C-Prs.

Form.	GBR	Content (kg/m^3)$^{(1)}$	$Al_2O_3{}^{(2)}$	Na_2O	Total $SO_3{}^{(3)}$	Free $SO_3{}^{(4)}$
C-Qpr	Qpr gravel	922	0.41%	0.7%	0.5%	0.18%
	Qpr sand	560	0.49%	1.3%	0.5%	0.12%
C-Prs	Prs gravel	978	0.20%	0.69%	0.4%	0.24%
	Prs sand	594	0.59%	0.23%	0.6%	0.13%

(1) Real RCA weight in 1 m^3 of concrete $<$ than quartz aggregate content in tab. 7
(2) Considered equal as molar content of bonded SO_3.
(3) Obtained by X-ray fluorescence test.
(4) From soluble sulphate measurement (tab. 3).

Table 14: Estimation of sulphates, aluminates and alkali in mortar formulations tab. 6 with added mortars from Yammmine et al. [12]

Form.	ϕ (%)	Cement$^{(1)}$ (kg/m^3)	$Al_2O_3{}^{(2)}$ (%)	$Fe_2O_3{}^{(2)}$ (%)	$Na_2O^{(2)}$ (%)	$SO_3{}^{(2)}$ (%)	$A_c^{(3)}$ (mol/m^3)	$S_c^{(3)}$ (mol/m^3)	S_c/A_c -	$[Na_0]^{(3)}$ (mol.l^{-1})
M-Ref	18.0%	513.2	5.28%	2.96%	0.8%	3.1%	361	320	0.89	$0.736^{(4)}$ / $2.09^{(5)}$
M-RF10	18.0%	459.1	5.28%	2.96%	0.8%	3.1%	328	304	0.93	$0.911^{(4)}$ / $2.26^{(5)}$
M-RF20	18.0%	405.6	5.28%	2.96%	0.8%	3.1%	296	288	0,97	$1.08^{(4)}$ / $2.42^{(5)}$
M-LF10	18.0%	460.6	5.28%	2.96%	0.8%	3.1%	324	300	0,92	$0.661^{(4)}$ / $2.01^{(5)}$
M-LF20	18.0%	408.3	5.28%	2.96%	0.8%	3.1%	287	279	0,97	$0.586^{(4)}$ / $1.93^{(5)}$
Ref	18%+4%*	492.7	5.28%	2.96%	0.8%	3.1%	347	191	0.55	0.71
Ref-SS	18%+4%*	492.7	5.28%	2.96%	0.8%	3.1%	347	295	0.85	$0.71^{(4)}$ / $1.86^{(5)}$
Qpr	38%	417.5	5.28%	2.96%	0.8%	3.1%	419	252	0.60	0.42
Qpr-SS	38%	417.5	5.28%	2.96%	0.8%	3.1%	419	252	0.81	$0.42^{(4)}$ / $0.89^{(5)}$
Prs	31%	445.4	5.28%	2.96%	0.8%	3.1%	397	255	0.64	0.47
Prs-SS	31%	445.4	5.28%	2.96%	0.8%	3.1%	397	349	0.88	$0.47^{(4)}$ / $1.1^{(5)}$

(1) Effective cement content.
(2) Content in cement only.
(3) Including amounts from recycled filler and sodium sulphate addition, see tab. 4; 5; 6.
(*) + 4% additional porosity as entrained air to adjust the estimated fresh density to the measured fresh density.
(4) Case N°1 default estimation: $[Na_0] = 2\ [Na_2O]$ only
(5) Case N°2 including sodium sulphate: $[Na_0] = 2\ [Na_2O] + 2\ [Na_2SO_4]$

3.5 Sample geometry impact on alkali lixiviation

Alkali lixiviation modelling requires defining a geometry for the modelled sample, an initial alkali concentration, which is obtained from tab. 12; 14, boundary conditions and a diffusion coefficient for concrete or mortar.

Computing diffusion is possible using finite element method, or with other numerical solving method by subdividing the domain. In some cases an analytical solution is possible, for example for a sphere or cylinder of an infinite height with a uniform diffusion coefficient and uniform boundary conditions [47]. Mortars have a prismatic geometry of $40\times40\times160\,mm^3$ and concrete have a cylindrical geometry of 110 mm diameter and 220 mm height (see § 2.2.3). The closest ideal geometry with an analytical solution to both mortar and concrete samples is a long cylinder having the same diameter than concrete cylinders (110 mm) or equal to the smallest edge of mortar prisms. An even simpler geometry is to consider a sphere instead of a long cylinder, but the drawbacks of this simplification will be a faster lixiviation than for the real sample geometry.

Equations (13) & (14) gives respectively the analytical solution of a sphere and a long circular cylinder given from Crank (1975) [47]. The concentration $C(r,t)$ is a function of two variables: r the radial position of the point and t the time elapsed since the start of diffusion. C_{ini} and C_{ext} are respectively internal and external initial concentration considered uniform. R_{ext} is the external radius, it corresponds to the radial position of the boundary. D is the diffusion coefficient of the sample, α_n are the roots of: $J_0(R_{ext}\alpha_n) = 0$; where $J_0(x)$ is the Bessel function of the first kind of order zero. $J_1(x)$ is the Bessel function of the first order.

$$C\,(r,t) = C_{ini} + (C_{ext} - C_{ini})\left(1 - \frac{2}{R_{ext}}\sum_{n=1}^{\infty}\frac{\exp\left(-D\,\alpha_n^2\,t\right)J_0\left(r\,\alpha_n\right)}{\alpha_n\,J_1\left(R_{ext}\,\alpha_n\right)}\right) \tag{13}$$

$$C\,(r,t) = C_{ini} + (C_{ext} - C_{ini})\,\frac{2R_{ext}}{\pi r}\sum_{n=1}^{\infty}\frac{(-1)^n}{n}\sin\frac{n\pi r}{n}\exp\left(\frac{-Dn^2\pi^2 t}{R_{ext}^2}\right) \tag{14}$$

Setting the right diffusion coefficient is not straightforward as little studies have measured diffusion coefficient of alkali ions like sodium, potassium or even hydroxide ions that are often associated to alkali ions. Otherwise, chloride diffusion have been well studied. Although the diffusion coefficient of chloride ions is not equal to that of alkali, we will assume that it is possible to use measurements of chloride diffusion coefficients to set the alkali diffusion coefficient as a model input parameter. Table 15 presents several measures of chloride diffusion coefficient in Portland cement pastes with a water-to-cement ratio of 0.5 drawn from the literature. Diffusion coefficient is about 4 to 8 $\times 10^{-12}$ $m^2.s^{-1}$. Furthermore, the national French Project ***Recybéton*** published results of chloride diffusion in natural and recycled aggregate concrete [15]. Results are presented in tab. 16, they show an increase in diffusion coefficient up to 80% when NA are replaced by RCA. At high resistance class C45/55, RCA did not impact the diffusion coefficient, for the reason that high resistance mixture is made of higher paste volumes and this makes aggregate inclusions unable to connect with each other, thus their effect will drastically decrease. In subsequent computations, the diffusion coefficient for all concretes and mortars with natural aggregates will be set to 5×10^{-12} $m^2.s^{-1}$ and the double will be set for RCA concretes (see tab. 17).

Table 15: Experimental measurements of chloride diffusion coefficient in ordinary Portland cement pastes for a water-to-cement ratio of 0.5. An average within the range [min - max] is provided in case several measurements are available.

Ref.	Diffusion coefficient D_{Cl^-} ($\times 10^{-12}$ $m^2.s^{-1}$)	T (°C)
[48]	4,47 [4,06 - 4,82]	25
[49]	5,45	25
[50]	7,80 [7,16 - 8,06]	25
[51]	7,84	25
[52]	6,81 [6,41 - 7,28]	23
[53]	8,24	[-]

Table 16: Chloride diffusion coefficient in natural aggregate and recycled aggregate concrete from Rougeau et al. [15].

Resistance class	Diffusion coefficient D_{Cl^-} ($\times 10^{-12}$ $m^2.s^{-1}$)		
	Natural aggregate	30% RCA	100% RCA
C25/30	23	24	29
C35/45	12	10	20
C45/55	7	5	6

Table 17: Alkali diffusion coefficient set for modelling DEF in concrete and mortar formulations.

Reference	D_{Na} ($\times 10^{-12}$ $m^2.s^{-1}$)
C-Ref	5
C-Qpr & C-Prs	10
M-Ref	5
M-RF10 & M-RF20	5
M-LF10 & M-LF20	5

Diffusion of alkali for C-Ref is applied using eq. 13 for a long cylinder of 11 cm diameter and eq. 14 for a sphere of 11 cm diameter assuming a constant external alkali concentration of $C_{\text{ext}} = 0.01$ mol.l^{-1}. Alkali concentration is plotted in fig. 6 for both cylindrical and spherical geometries at five radial positions, $r = 1$; 2.5; 3.5; 4 and 5 cm. For the two geometries, alkali concentration decreases extremely slowly near the center with [Na] > 0.5 mol.l^{-1} at $r = 1$ cm after 500 days. At low depth ($r = 5$ cm) the concentration decreases extremely fast reaching 0.25 mol/l^{-1} in 100 days for both geometries. Alkali concentration is highly influenced by the depth and to a lesser extent by the geometry of the sample. In most cases there is little need for a high accuracy estimation of the lixiviation kinetics as just the average remaining quantity of alkali concentration is required. In such cases, it is possible to adopt the simplified representation of the lixiviation by the diffusion in a sphere. In what follows, only long cylindrical shapes will be considered. Moreover, the alkali diffusion may be altered by adsorbed alkali on C-S-H as it behaves as a buffer alkali tank, which decreases the lixiviation kinetics. The apparent diffusion coefficient will be $D_{\text{app}} = \frac{D_{\text{eff}}}{1+k}$ where D_{eff} is the effective diffusion coefficient of the medium without any adsorption effect and k is the slope of the binding isotherm: $k = C_{\text{ad}}/C_{\text{f}}$ with C_{ad} the adsorbed concentration and C_{f} the free concentration. According to Sellier & Multon [18], when heat curing occurs at early age, the adsorption impact can be neglected due to small concentration of C-S-H at early age.

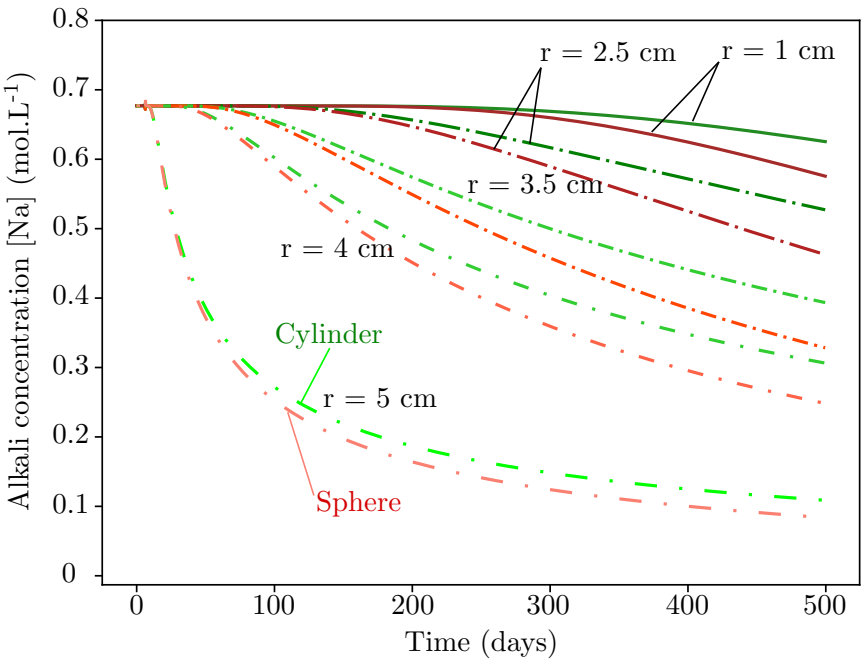

Figure 6: Alkali concentration evolution computed for C-Ref concrete with a coefficient of diffusion of $D = 5 \times 10^{-12}$ m^2.s^{-1}. Two ideal geometries are considered, in red a sphere of 11 cm diameter and in green a long cylindrical sample of 11 cm diameter. Five curves are plotted for each geometry at $r = 1$; 2.5; 3.5; 4 and 5 cm with r the radial position in the sphere and in the cylinder.

4 Model results and comparison to experiments

Chemical content simulation using the equations in § 3.2 is guided by thermal, alkali and saturation physical states. Temperature evolution shown in fig.7-(a) is applied on all formulations, it is determined according to the curing cycle in § 2.2.4. Fig.7-(b) illustrates the chemical content evolution at early age. During the curing phase that is green highlighted, the amount of monosuphate decreases while free sulphates increase and free aluminates increase and decrease due to fixation. Alkali concentration is determined analytically using eq. (13) of a long cylinder of 11 cm for concrete and 4 cm for mortars immersed in a weak alkaline solution of a constant concentration of $C_{\text{ext}} = 0.01\,\text{mol.l}^{-1}$. Saturation is considered equal to 100% as all samples are stored in water.

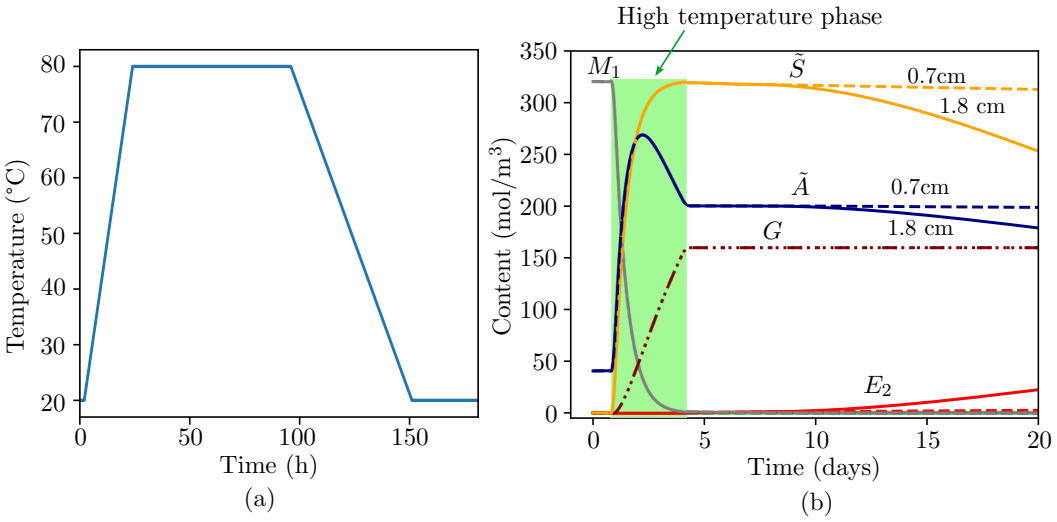

Figure 7: Temperature evolution applied on all formulations in (a) and chemical content evolution at early ages for M-Ref (b).

4.1 Modeled chemical content evolution

Content evolution of primary and delayed ettringite, monosulphate, hydrogarnet, free aluminates and free sulphates of the three concretes and three of the 5 mortars (M-Ref, M-RF20 and M-LF20) are shown in fig. 8 for two positions R_1 and R_2. Chemical content evolution of M-RF10 and M-LF10 are respectively close to M-RF20 and M-LF20. Radii values are chosen to represent DEF evolution for two different cases, the first located at shallow depth and the second close to the core of the sample (see fig. 6). For concrete cylinders ($D = 11\,\text{cm}$), $R_1 = 4\,\text{cm}$ and $R_2 = 1.5\,\text{cm}$. For mortar cylinders ($D = 4\,\text{cm}$), $R_1 = 1.8\,\text{cm}$ and $R_2 = 0.7\,\text{cm}$.

Free sulphates and free aluminates are at maximum concentration after the curing period, they are the products of sulfoaluminates dissolution. All studied formulations have $S_c/A_c < 1$, thus the only available sulfoaluminate at $t = 0$ is M_1, while $E_1(0) = E_2(0) = 0$. After heat curing, a small amount of monosulphates remains in some formulations, mostly in C-Qpr and C-Prs. This happens when initial alkali concentration is not sufficiently elevated and / or when the curing cycle does not last enough to consume all sulfoaluminates. Indeed, the activation coefficients C_d^T and C_d^C

(tab. 10) behave as follow: C_d^T is equal to 0 when $T < T_{th,d}$ (≈ 70°C), and increases exponentially at higher temperature while C_d^C increases linearly with the alkali concentration. Thus, high temperature and alkali concentration increase sulfoaluminate dissolution.

DEF kinetics in C-Ref is slower compared to C-Qpr and C-Prs since alkali concentration in C-Ref is higher than in the two recycled aggregate concrete and the diffusion coefficient was assumed to be in recycled aggregate concrete the double of that of C-Ref. Thus initial alkali concentration is higher in C-Ref and remains longer at high level in comparison with C-Qpr and C-Prs. Measured expansion values in fig. 3 shows that C-Ref exhibited a significant expansion with a maximum 0.18 %, but not C-Qpr nor C-Prs (≈ 0.03 %). C-Ref reached 95% of maximum expansion in 180 days but modelled maximum expansive volume is reached in about 300 to 500 days. C-Ref simulation have a slower kinetics in comparison with its experimental expansion curve. Slower kinetics is probably the result of underestimated diffusion coefficient or the result of assuming a constant diffusion coefficient with respect to damage evolution. If a higher diffusion coefficient is taken in concretes and mortars then modelled kinetics in mortars are faster than the experimental one. Even though the DEF simulation kinetics is not faithfully reproduced, when the reaction ends, the same content of all species will be obtained regardless of the depth and the speed of DEF. Uniform content of all species is obtained at the end of DEF if the heat curing cycle and final alkali concentration are uniform over the whole sample. Consequently, the final delayed ettringite content is the most interesting output to analyse. C-Ref have the lowest final E_2 value equal to 64 mol/m^3, C-Qpr and C-Prs have close final E_2 values about 84 - 87 mol/m^3. This result can not explain the measured expansion as C-Ref is the only concrete that exhibited significant expansion. The occurrence of ettringite after curing requires a restrained porous volume to induce expansion. Porosity measurement in fig. 5 shows that recycled aggregate concrete are highly porous. Moreover, the production of ettringite is the result of residual monosulphate consumption, that should be considered as a disappearing volume to be replaced with ettringite.

Model results for the 3 mortar formulations show a highest E_2 content for M-Ref, about 107 mol/m^3. This amount decreases with substitution by fines in recycled filler mortars and even more in limestone filler mortars.

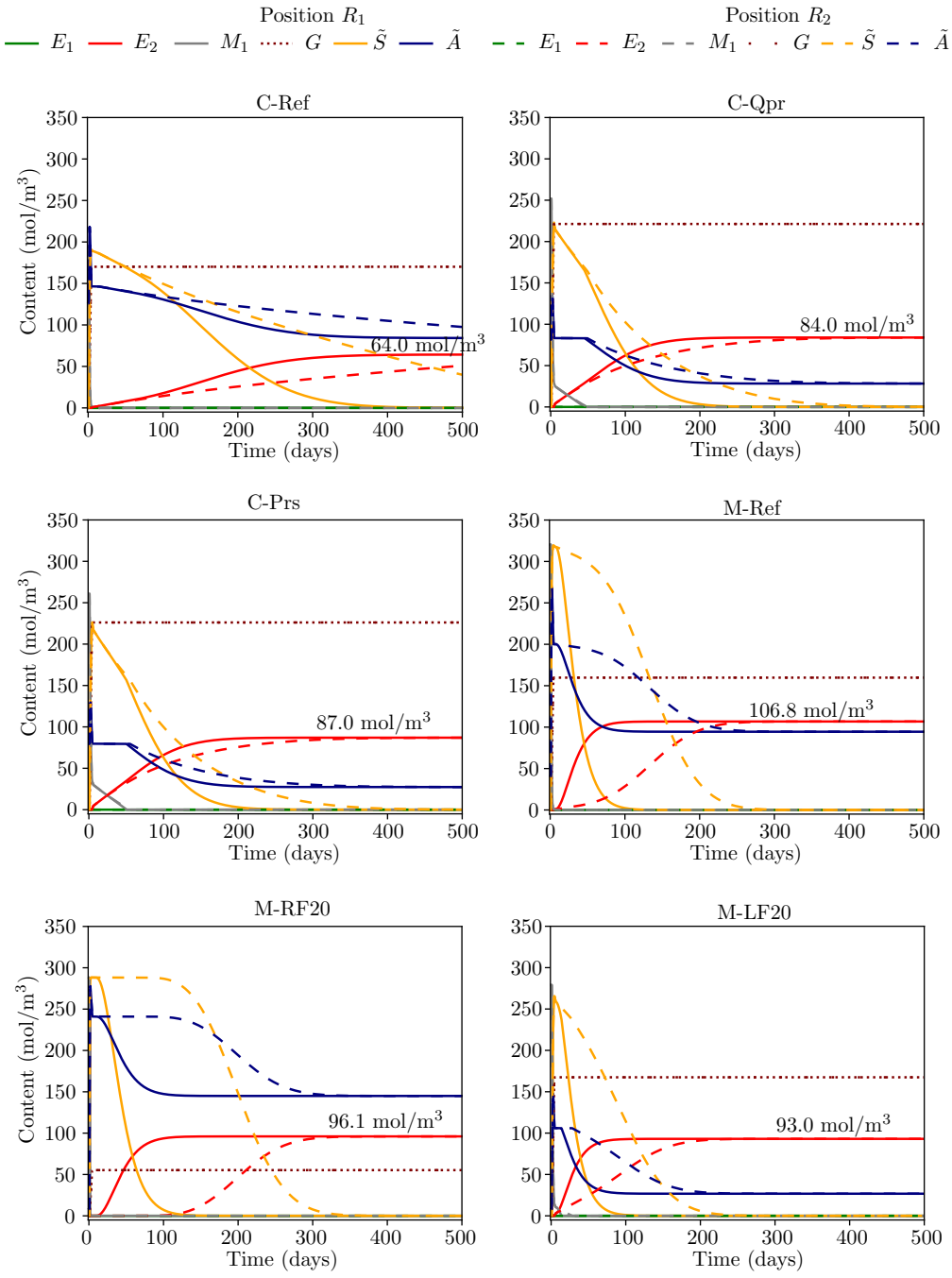

Figure 8: modelled content evolution of chemical compounds in C-Ref, C-Qpr, C-Prs, M-Ref, M-RF20 and M-LF20 in a long cylinder of 11 cm diameter for concretes and 4 cm diameter for mortars on a period of 500 days. $R_1 = 4$ cm; $R_2 = 1.5$ cm for concrete cylinders and $R_1 = 1.8$ cm; $R_2 = 0.7$ cm for mortar cylinders.

4.2 Expansive volume and axial expansion

The swelling due to DEF is the consequence of the appearance of a volume within the cement matrix which consists of ettringite. Precipitating ettringite under pressure requires elevated activity of ettringite reagent species, which appears in some pores and can dissipate through diffusion to free pores. When ettringite volume fails to dissipate completely or partially, it will push and develop an expansion. When the diffusion rate is greatly slower than the production rate, the expansive volume will fill the part of porosity in which it is produced and then trigger an expansion.

The expansive volume is defined from the chemical model by the following equation:

$$\Phi_{\text{DEF}} = \langle \Delta V_{M_1} + \Delta V_{E_2} \rangle^+ \tag{15}$$

In eq.(15), $\Delta V_{M_1}(t)$ and $\Delta V_{E_2}(t)$ are the variation of monosulphate and delayed ettringite volume respectively at time t from the end of the curing cycle at time $t_{\text{heat end}}$, with $t \geq t_{\text{heat end}}$. $\Delta V_{M_1}(t) = V_{M_1}(t) - V_{M_1}(t_{\text{heat end}})$; $\Delta V_{E_2}(t) = V_{E_2}(t) - V_{E_2}(t_{\text{heat end}})$. $\langle \diamondsuit \rangle^+$ is the positive part of $\diamondsuit$. The positive part eliminates the possibility of a negative expansive volume, which corresponds instead to an increase in porosity. This happens at the beginning of the precipitation phase, since the volume of consumed monosulphate is higher than that of the delayed ettringite produced. The expansive volume can be expressed as a function of the variation of ettringite and monosulphate contents as :

$$\Phi_{\text{DEF}} = \langle V_{\text{Afm}}\, \Delta M_1 + V_{\text{Aft}}\, \Delta E_2 \rangle^+ \tag{16}$$

where V_{Afm} and V_{Aft} are the molar volumes of monosulphate and ettringite respectively. Molar volume values are taken the same as Sellier & Multon [18]; $V_{\text{Afm}} = 254$ cm^3/mol and $V_{\text{Aft}} = 715$ cm^3/mol, as measured by [54]. ΔM_1 and ΔE_2 are the variations of the molar content of monosulphate and delayed ettringite from the end of the curing cycle.

As a first crude assumption, in the case of a whole conversion of expansive volume into an isotropic expansion, the axial expansion of the material would be equal to 1/3 the expansive volume produced:

$$\text{Axial expansion}^* = \frac{1}{3}\Phi_{\text{DEF}} \tag{17}$$

**only if all the expansive volume were converted in an isotropic expansion.*

The assumption eq. (17) was considered by Sellier & Multon for the fitting procedure of the kinetic parameters of the model. However, it is likely invalid in general and a poromechanical modeling should be used to estimate the actual expansion. In particular, no expansion can be observed despite a massive production of ettringite in the case of high porosity materials such as cementitious materials with air-entraining agents [55] or formulated with RCA [13, 12]. We further investigate this aspect in what follows.

The third of the expansive volume as per eq. (17) is plotted for concrete and mortar formulations in fig. 9. The maximum measured expansion is compared to the maximum modelled third of the expansive volume and the difference between the two is shown as a non expansive DEF. In both concrete and mortar results, the assumption eq. (17) of an expansion equal to one third of the expansive volume is not valid. The non expansive DEF is defined as one third the volume filled by ettringite that did not induce an expansion. A small augmentation in the modelled expansive volume is noticed when considering alkali from sodium sulphate (case N°2). Non expansive DEF is about 1.8% - 2% in all mortars, this means that non expansive ettringite filled the same pore volume

in the 5 mortars. Those mortars have many common important characteristic that explains this result. Cement, sand and porosity ($\approx 18\%$) are unchanged between the 5 mortars. On the other hand, concretes are made with different aggregates, having different porosity. Non expansive DEF in RCA concrete is almost equal to the third of the modelled expansive volume. This means that all formed delayed ettringite did not develop an expansion. Our interpretation is that a higher amount of expansive volume is needed in RCA concrete to induce an expansion due to their elevated porosity, as also found by [13].

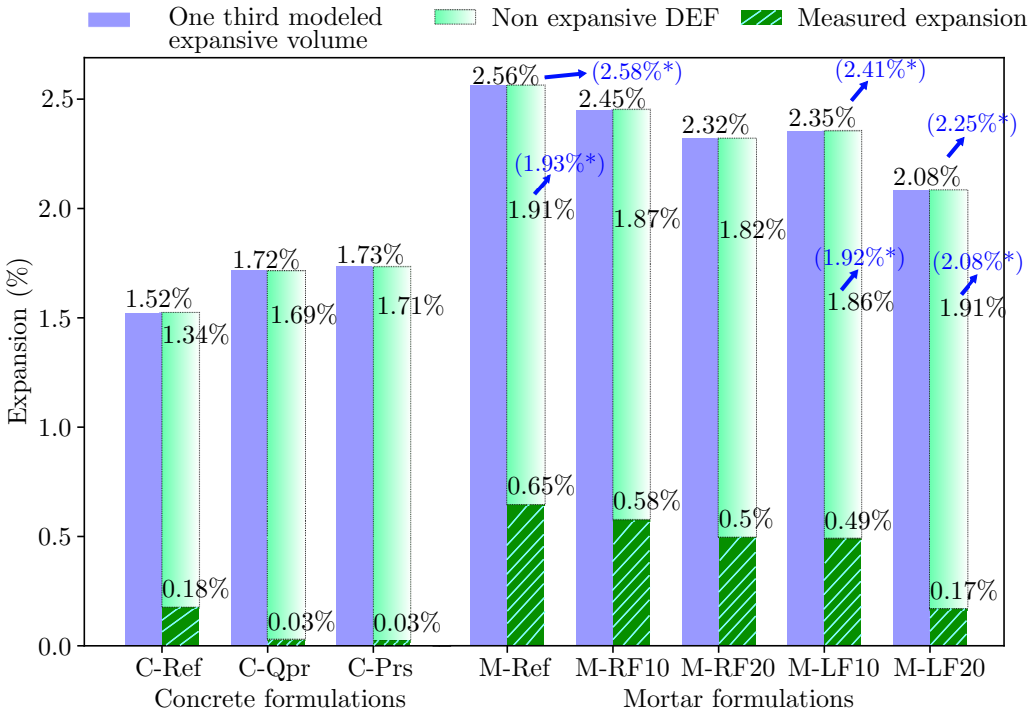

Figure 9: Comparison between the modelled expansive volume and the maximum measured expansion for the three concrete C-Ref, C-Qpr and C-Prs and mortars M-Ref, M-RF10, M-RF20, M-LF10, M-LF20. * are modelled expansive volumes for M-Ref, M-LF10 and M-LF20 when alkali content from sodium sulphate is counted (case N°2). No increase in expansive volume result is obtained for M-RF(10 & 20) in case N°2.

Modelled expansive volumes for Yammine (2020) mortars [12] are shown in fig. 10. Counting alkali from sodium sulphate increases a lot the modelled expansion in recycled sand based mortars but not in reference mortar. Qpr-SS and Prs-SS third of modelled expansive volume increased from 1.2% to 2.6% and from 2.0% to 2.8% respectively. When initial alkali content is not sufficiently elevated, monosulphate is dissolved partially and reduces the modelled expansive volume which is the case of the recycled sand based mortars. Alkali concentration impact on the modelled expansive volume is detailed in § 4.3. Qpr-SS and Prs-SS have a porosity of 38% and 35% respectively and they have a maximum expansive DEF volume (case N°2) of $3\times2.74\%$ and $3\times2.8\%$. Consequently, the amount of expansive DEF volume has filled 21% to 25% of their porosity. On the other hand, Ref-SS and M-Ref have an expansive volume of $3\times2.38\%$ and $3\times2.58\%$ which is equivalent to 39% and 43% of their porous volume. Elevated

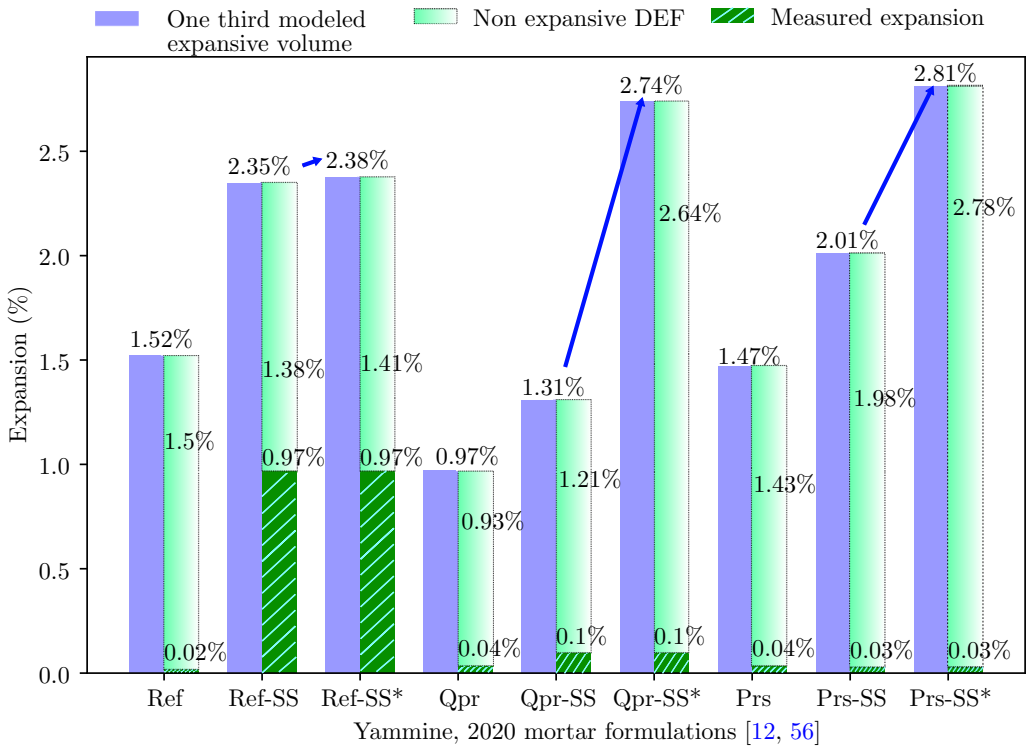

Figure 10: Comparison between the modelled expansive volume and the maximum measured expansion for Yammine (2020) mortars. Formulations with * counts alkali content from sodium sulphate (case N°2).

porosity in recycled aggregate mortars and concretes may decrease ettringite crystallization pressure by fast redistribution of the reagents through the porosity, and reduce drastically the swelling.

Species evolution with time is not shown for the sake of simplicity, but it should be noted that ettringite precipitation is extremely delayed when sodium sulphate is counted in alkali concentration, which does not reflect the real development of DEF. Sodium sulphate is largely used as a DEF amplifier and has not been reported as having an important delaying effect on DEF development [27, 23, 57, 42].

According to Scherer [16], higher hydroxide concentration impacts negatively ettringite superconcentration ratio. Thus elevated hydroxide concentration enhances ettringite dissolution, while on the contrary, decreasing $[OH^-]$ triggers precipitation. However in the model of Sellier & Multon [18], alkali concentration plays the major role in enhancing dissolution. Sodium and potassium where proven to enhance sulphate adsorption on C-S-H, this decreases sulphate availability for ettringite crystallization.

4.3 Effect of alkali concentration on DEF model

Alkali concentration impacts the expansive volume as shown in the previous section. Low alkali content decreases the dissolution which decreases primarily the expansive volume and secondarily the delayed ettringite volume. The latter case is not noticed in this study, produced free sulphates are sufficient to convert all monosulphate to delayed ettringite. In this section the Volume Growth Factor is introduced as the ratio between

the expansive volume defined in eq. (16)) and the produced delayed ettringite:

$$\mathrm{VGF} = \frac{\langle V_{\mathrm{Afm}}\,\Delta M_1 + V_{\mathrm{Aft}}\,\Delta E_2\rangle^+}{\langle V_{\mathrm{Aft}}\,\Delta E_2\rangle^+} = \frac{\Phi_{\mathrm{DEF}}}{\langle V_{\mathrm{Aft}}\,\Delta E_2\rangle^+} \tag{18}$$

The VGF, the initial alkali concentration and the maximum DEF content are shown in fig. 11 - 12. A VGF of 100% represents a complete production of ettringite from free species (sulphates and aluminates) which results in a maximum expansion effect for the same amount of produced ettringite.

The VGF is impacted by alkali content and by curing conditions which are identical for all formulations. Consequently VGF difference between formulations in this study are the consequence of the difference in initial alkali content. Mortar and concrete formulations results in fig. 11 - 12 show that if alkali content is > 0.7 mol.l^{-1}, the VGF is $\approx 100\%$. The VGF decreases drastically between 0.7 and 0.4 mol.l^{-1}. For an initial alkali content of 0.4 mol.l^{-1}, the expansive volume decreases more than 50% which is the case of recycled sand mortars "Qpr" and "Prs". The same effect holds for "Qpr-SS" and "Prs-SS" in case N°1.

When sodium sulphate is not counted, recycled aggregate concrete and recycled sand mortars have low initial alkali concentrations due to their elevated porosity. Alkali amounts are diluted in a higher solution volume that saturates the pore voids. SEM observations of the samples confirm the presence of DEF products in the porosity, as in our previous work [12]. Thus, considering the right amount of alkali content when sodium sulphate is used is an important factor only if alkali content from cement is not sufficiently elevated for dissolving sulfoaluminates.

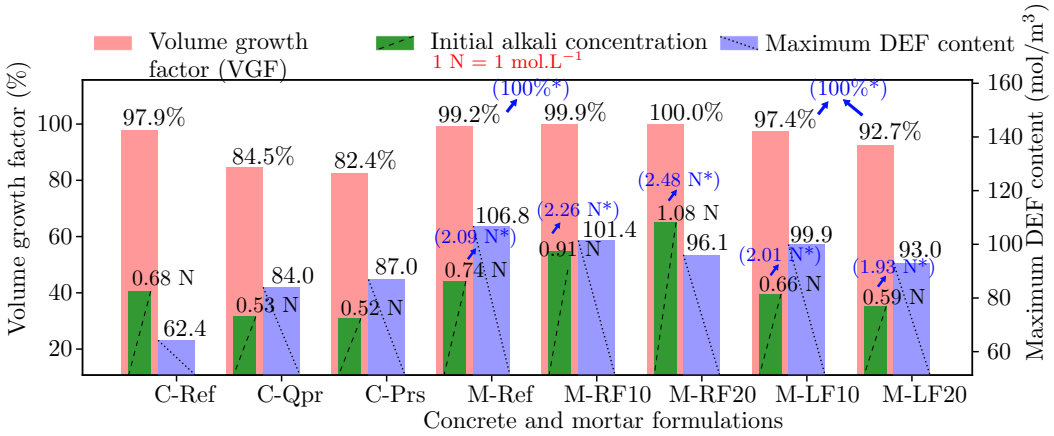

Figure 11: Results of the Volume Growth Factor (VGF), the maximum DEF content and the initial alkali content for concrete formulations: C-Ref, C-Qpr, C-Prs and mortars: M-Ref, M-RF(10 & 20) and M-LF(10 & 20). * are results alkali content from sodium sulphate (case N°2).

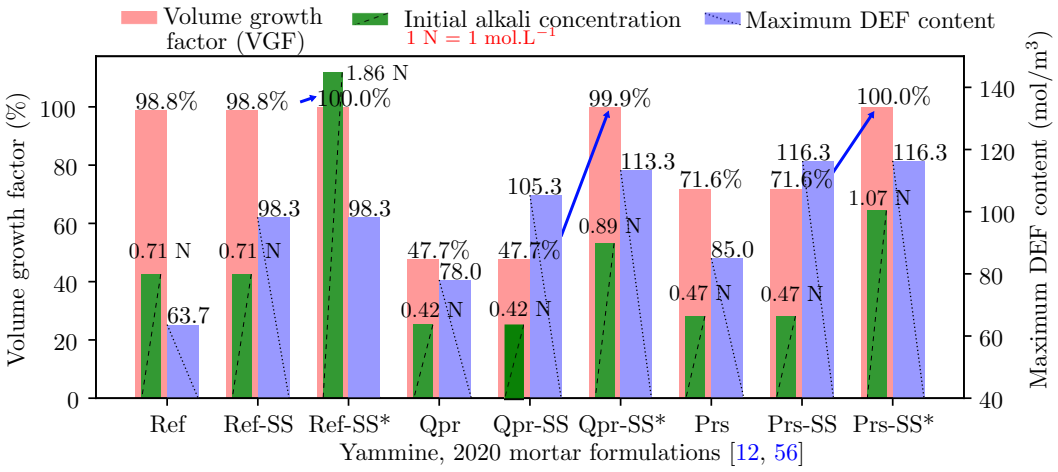

Figure 12: Results of the Volume Growth Factor (VGF), the maximum DEF content and the initial alkali content for Yammine (2020) mortar formulations.

4.4 Assessment of the predictive capacity of the model: effect of the porosity filling ratio

The DEF chemical model was fitted using several experimental results. Fig. 13 shows the studies [58, 59, 60, 61] that have been used by Sellier & Multon [18] to fit and validate the model assuming eq. (18). Experimental results of mortars and concretes presented in this study are also added, some of the measured expansions do not have any correlation with the model results. Fig. 14 shows the correlation between the estimated expansive volume – porosity fraction and the maximum measured expansion for the studied formulations. Uncorrelated results are mostly recycled aggregate mortars and concretes having an expansive volume to porosity fraction less than 30%. Elevated porosity needs to be sufficiently filled with ettringite, otherwise the expansive pressure decreases and the swelling is impeded. This effect has been considered in the poro-mechanical model of Sellier & Multon [18], in which a volume Φ^v_{DEF} is to be filled in a specimen before damage occurs. A similar coefficient: $\beta\phi^0$ was taken by Bary et al. [62], with ϕ^0 the initial porosity and β the fraction of the large pores to be filled with ettringite. β values were adjusted to experimental results and they were close to 0.7 (70%).

A correlation between the modelled expansive volume and the maximum measured expansion in fig. 13 is found for the mortars of tab. 6 (M-Ref, M-RF10, M-RF20, M-LF10 and M-LF20). Those mortars were made using the same standardised siliceous sand and cement. The only difference is in their fillers type and its content. The correlation equation has a slope of 0.95 which is very close to one. The y-intercept is 1.9%, thus a porous volume of 1.9%×3 = 5.7% was filled in all formulations by the same volume of non expansive ettringite. This volume is equal to 32% of the mortars porosity. The latter results of 32% is different from the indirectly fitted values of β (70%) found by Bary et al. [62]. As a consequence, the results show that the chemical model of Sellier & Multon can not predict directly the expansion of mortars or high porosity concretes, but can be used to obtain an expansive volume that is partially converted into an expansion. The mortars used in this study (tab. 6) and from Yammine (2020) show that the expansive volume to porosity fraction should be at least 30%,

otherwise there is a low possibility for expansion development. Consequently, predicting the maximum expansion from the maximum expansive volume may be possible if the minimum expansive volume that induces damage is known in advance.

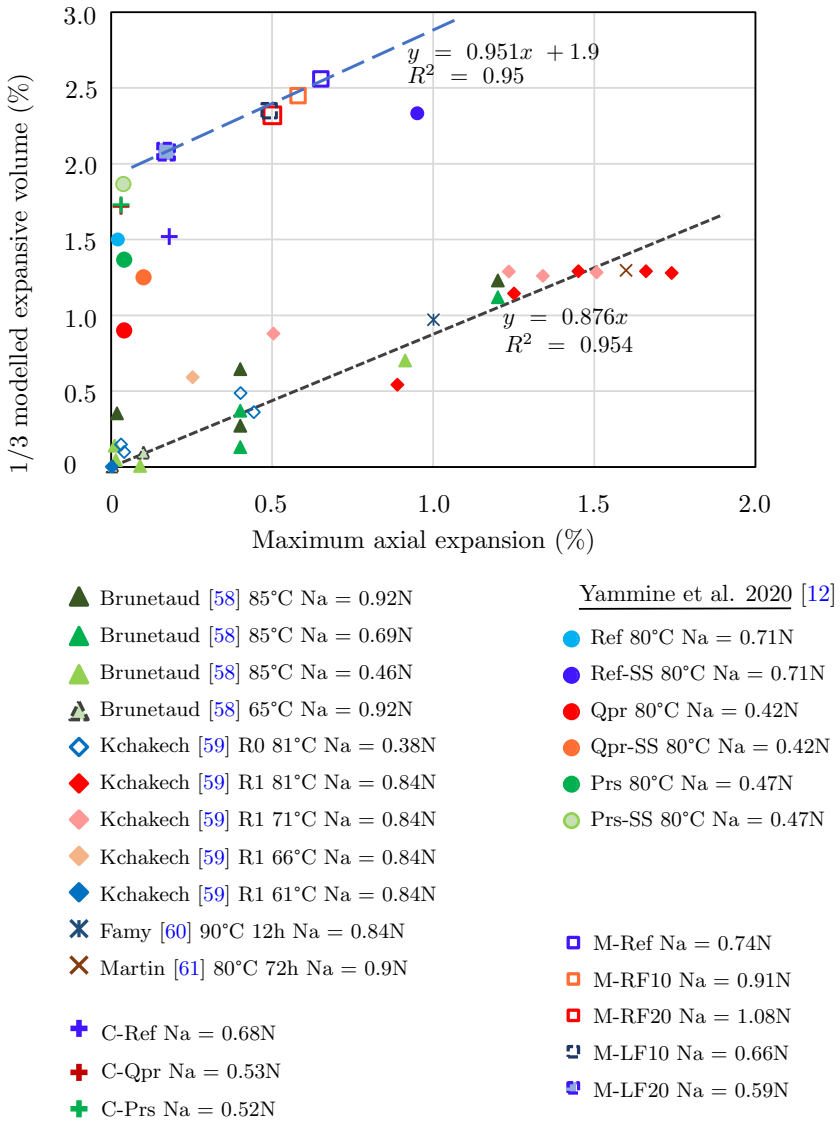

Figure 13: Comparing the maximum axial expansion with the third of the predicted expansive volume using Sellier & Multon model [18].

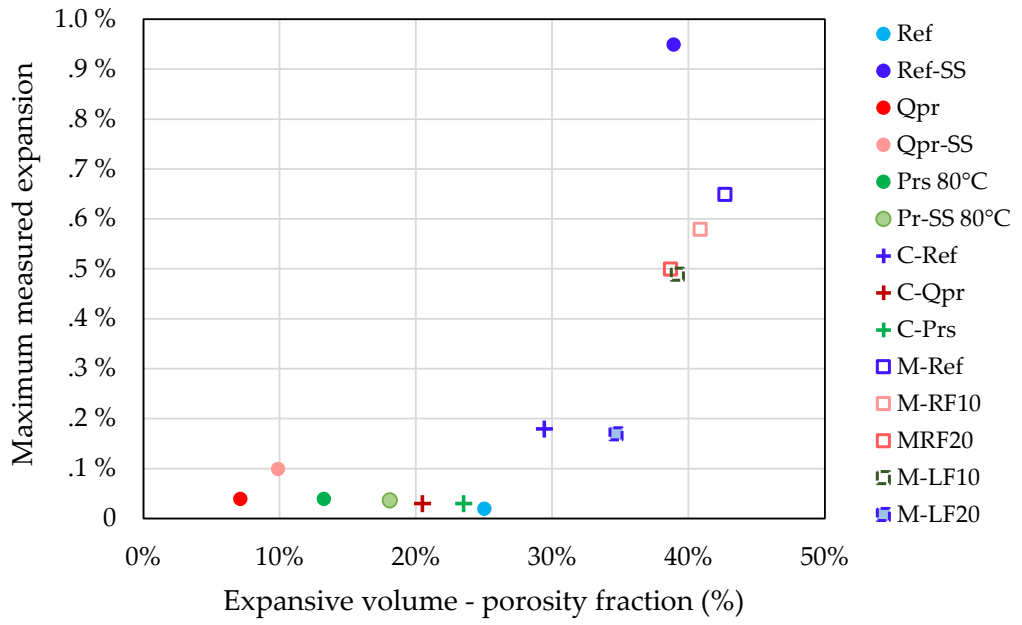

Figure 14: Correlation between the expansive volume - porosity fraction and the maximum measured expansion.

5 Conclusion

The effect of using recycled aggregate and recycled filler in concrete and mortars on delayed ettringite formation is studied experimentally. Three concrete formulations, one using siliceous aggregate as a control group and two others using two different RCA, and five standardized mortars have been monitored for over one year. One control group of mortar formulation had no additions and was compared with four mortar formulations, two with recycled filler and two others with limestone filler both at 10% and 20%. Sodium sulphate was added to all mortars to enhance DEF. All concrete and mortars were heat cured and conserved in water. Expansion measurements were compared to estimated modelled results using Sellier & Multon [18] chemical model. Moreover, additional mortar results from Yammine (2020) [12] study are added to the current study to investigate more precisely the behaviour of the model. Experimental and modelling results lead to the following conclusions:

RCA concretes did not develop expansion ($< 0.04\%$) in comparison with natural siliceous concrete ($\approx 0.2\%$). These results agree with Yammine (2020) [12] study of DEF in recycled sand based mortars. Elevated porosity due to RCA usage is responsible of limiting DEF. Although elevated porosity seems beneficial to inhibit DEF, it can be detrimental for other pathologies such at external sulfate attack, chloride penetration or carbonation, elevated porosity as it usually implies a faster transport of aggressive ions.

Recycled filler has shown a little inhibiting effect on DEF expansion. A higher inhibiting effect is shown with limestone filler. Recycled filler contained 0.9% of soluble sulphates and was very rich in alkali (2.76%). If the recycled filler had higher sulphate content it would induce higher expansion. This study can not confirm the safety of using recycled filler as a replacement for limestone filler. However, it will be less likely

to DEF to develop if sulphates and alkali contents in the recycled filler are lower than in the used cement.

Model results show that the expansive volume produced in recycled sand mortars and concrete is not sufficiently elevated to develop an expansion. Mortars and concrete that developed expansion had mostly an expansive volume greater than 30% of their porosity. Those who had an expansion higher than 0.5% had an expansive volume close to 40% of their porous volume. The five mortars in this study showed a linear correlation of their maximum measured axial expansion and their corresponding modelled expansion results. The volume of non expansive ettringite was constant regardless of the differences in the formulations and was about 1/3 the mortar porous volume. Consequently, a minimum expansive volume fraction is to be determined in order to predict the maximum expansion. In this study, the minimum volume was found to be 30% for mortars. Further studies are required to establish a link between different concrete and mortar formulations and the minimum expansive volume by changing formulation parameters such as the type of binder and the water to cement ratio.

Declaration of Competing Interest

The authors declare that they have no known competing financial interests or personal relationships that could have appeared to influence the work reported in this paper.

Acknowledgment

The authors would like to acknowledge: The Algerian-French cooperation project Tassili 19MDU216. The financial support of the Polish National Agency for Academic Exchange under the International Academic Partnership Program: PPI/APM/2018/1/00027 E-mobility and sustainable materials and technologies EMMAT. The financial support of the French Ministry of Higher Education.

The authors thank Philippe Leroy of the GeM laboratory for his help on the technical aspects of this work.

This article is dedicated to the memory of Alexandre Yammine, first author, who tragically passed away shortly after the submission of the article. May he rest in peace.

References

[1] N. Garcia-Troncoso, L. Li, Q. Cheng, K. H. Mo, and T.-C. Ling, "Comparative study on the properties and high temperature resistance of self-compacting concrete with various types of recycled aggregates," *Case Studies in Construction Materials*, vol. 15, p. e00678, 2021.

[2] B. C. Mendes, L. G. Pedroti, C. M. F. Vieira, M. Marvila, A. R. Azevedo, J. M. Franco de Carvalho, and J. C. L. Ribeiro, "Application of eco-friendly alternative activators in alkali-activated materials: A review," *Journal of Building Engineering*, vol. 35, p. 102010, 2021.

[3] N. Damrongwiriyanupap, T. Srikhamma, C. Plongkrathok, T. Phoo-ngernkham, W. Sae-Long, S. Hanjitsuwan, P. Sukontasukkul, L. yuan Li, and P. Chindaprasirt, "Assessment of equivalent substrate stiffness and mechanical properties of sustainable alkali-activated concrete containing recycled concrete aggregate," *Case Studies in Construction Materials*, vol. 16, p. e00982, 2022.

[4] O. Zaid, F. M. Mukhtar, R. M-García, M. G. El Sherbiny, and A. M. Mohamed, "Characteristics of high-performance steel fiber reinforced recycled aggregate concrete utilizing mineral filler," *Case Studies in Construction Materials*, vol. 16, p. e00939, 2022.

[5] N. Oikonomou, "Recycled concrete aggregates," *Cement and Concrete Composites*, vol. 27, no. 2, pp. 315–318, 2005. Cement and Concrete Research in Greece.

[6] S. Delvoie, Z. Zhao, F. Michel, and L. Courard, "Market analysis of recycled sands and aggregates in northwest europe: drivers and barriers," *IOP Conference series: Earth and Environmental Science*, vol. 225, pp. 1–8, 2019.

[7] C. Lawrence, "Mortar expansions due to delayed ettringite formation. effects of curing period and temperature," *Cement and Concrete Research*, vol. 25, pp. 903–914, May 1995.

[8] H. Taylor, C. Famy, and K. Scrivener, "Delayed ettringite formation," *Cement and Concrete Research*, vol. 31, pp. 683–693, May 2001.

[9] S. Kelham, "The effect of cement composition and fineness on expansion associated with delayed ettringite formation," *Delayed Ettringite Formation*, vol. 18, pp. 171–179, Jan. 1996.

[10] R. V. Silva, J. d. Brito, and R. K. Dhir, "Properties and composition of recycled aggregates from construction and demolition waste suitable for concrete production," *Construction and Building Materials*, vol. 65, pp. 201 – 217, 2014.

[11] NF EN 12620+A1, "Aggregates for concrete." AFNOR - European standard - French standard, June 2008.

[12] A. Yammine, N. Leklou, M. Choinska, F. Bignonnet, and J.-M. Mechling, "DEF damage in heat cured mortars made of recycled concrete sand aggregate," *Construction and Building Materials*, vol. 252, p. 119059, Aug. 2020.

[13] C. Colman, D. Bulteel, S. Rémond, Z. Zhao, and L. Courard, "Valorization of fine recycled aggregates contaminated with gypsum residues: Characterization and evaluation of the risk for secondary ettringite formation," *Materials*, vol. 13, no. 21, 2020.

[14] C. Colman, D. Bulteel, V. Thiery, S. Rémond, F. Michel, and L. Courard, "Internal sulfate attack in mortars containing contaminated fine recycled concrete aggregates," *Construction and Building Materials*, vol. 272, p. 121851, 2021.

[15] P. Rougeau, L. Schmitt, J. Nai-Nhu, A. Djerbi, M. Saillio, E. Ghorbel, J.-M. Mechling, D. Bulteel, M. Cyr, A. Lecomte, N. Leklou, R. Trauchessec, I. Moulin, T. Lenormand, and O. Amiri, *Propriétés liées à la durabilité*, ch. 12, pp. 273–321. De Larrard F. et Colina H. (Dir.), Le béton recyclé. Ouvrages Scientifiques, OSI4., Marne-la-Vallée: Ifsttar, 2018.

[16] R. J. Flatt and G. W. Scherer, "Thermodynamics of crystallization stresses in DEF," *Cement and Concrete Research*, vol. 38, no. 3, pp. 325–336, 2008.

[17] M. Salgues, A. Sellier, S. Multon, E. Bourdarot, and E. Grimal, "DEF modelling based on thermodynamic equilibria and ionic transfers for structural analysis," *European Journal of Environmental and Civil Engineering*, vol. 18, no. 4, pp. 377–402, 2014.

[18] A. Sellier and S. Multon, "Chemical modelling of Delayed Ettringite Formation for assessment of affected concrete structures," *Cement and Concrete Research*, vol. 108, pp. 72 – 86, 2018.

[19] A. Yammine, F. Bignonnet, N. Leklou, M. Choinska, and T. Stryszewska, "Micromechanical modelling of damage induced by delayed ettringite formation," in *10th International Conference on Fracture Mechanics of Concrete and Concrete Structures*, FraMCoS-X, (Bayonne, France), 2019.

[20] A. Yammine, F. Bignonnet, N. Leklou, and M. Choinska, "Micromechanical modelling of damage induced by delayed ettringite formation in concrete," in *MATBUD'2020 – Scientific-Technical Conference: E-mobility, Sustainable Materials and Technologies*, vol. 322, p. 01037, 2020.

[21] NF EN 206+A1, "Concrete - specification, performance, production and conformity." AFNOR - European standard - French standard, 2016.

[22] NF P18-594, "Aggregates - test methods on reactivity to alkalies." AFNOR - European standard - French standard, 2015.

[23] Y. Amine, N. Leklou, and O. Amiri, "Effects of Ternary Cements with Limestone Filler on DEF in Concrete," *ACI Symposium Publication*, vol. 320, 2017.

[24] NF EN 1097-6, "Tests for mechanical and physical properties of aggregates - Part 6: determination of particle density and water absorption." AFNOR - European standard - French standard, Jan. 2014.

[25] NF EN 1744-1, "Tests for chemical properties of aggregates - Part 1: chemical analysis." AFNOR - European standard - French standard, Feb. 2014.

[26] LCPC, "Méthode d'essai LPC n°37 : Essai de granulats. détermination des alcalins solubles dans l'eau de chaux," 1993.

[27] N. Leklou, V.-H. Nguyen, and P. Mounanga, "The effect of the partial cement substitution with fly ash on Delayed Ettringite Formation in heat-cured mortars," *KSCE Journal of Civil Engineering*, vol. 21, no. 4, pp. 1359–1366, 2017.

[28] W. Deboucha, N. Leklou, A. Khelidj, O. Plé, and U. J. Alengaram, "Combination effect of limestone filler and slag on delayed ettringite formation in heat-cured mortar," *Journal of Materials in Civil Engineering*, vol. 32, no. 3, p. 04019365, 2020.

[29] G. Escadeillas, J.-E. Aubert, M. Segerer, and W. Prince, "Some factors affecting delayed ettringite formation in heat-cured mortars," *Cement and Concrete Research*, vol. 37, no. 10, pp. 1445–1452, 2007.

[30] GranDuBé, "Essai LPC N°59, réactivité d'une formule de béton vis-à-vis d'une réaction sulfatique interne," in *GranDubé, Grandeurs associées à la Durabilité des Bétons* (G. Arliguie and H. Hornain, eds.), ch. I.4, pp. 271–290, 75007 Paris: Presses de l'école nationale des Ponts et chaussées, 2007.

[31] NF EN 196-1, "Methods of testing cement — Part 1: Determination of strength." AFNOR - European standard - French standard, Sept. 2016.

[32] NF EN 1008, "Specification for sampling, testing and assessing the suitability of water, including water recovered from processes in the concrete industry, as mixing water for concrete." AFNOR - European standard - French standard, July 2003.

[33] NF EN 12350-1, "Testing fresh concrete - Part 1: sampling and common apparatus." AFNOR - European standard - French standard, June 2019.

[34] NF EN 12390-1, "Testing hardened concrete - Part 1: Shape, dimensions and other requirements for specimens and moulds." AFNOR - European standard - French standard, Nov. 2012.

[35] NF EN 12390-2, "Testing hardened concrete - Part 2: making and curing specimens for strength tests." AFNOR - European standard - French standard, June 2019.

[36] FD P 18-457, "Concrete — Implementation guide for test methods." AFNOR - French standard, 2005.

[37] NF EN 12350-2, "Testing fresh concrete - Part 2: slump test." AFNOR - European standard - French standard, June 2019.

[38] NF P18-459, "Concrete - testing hardened concrete - testing porosity and density." AFNOR - French standard, 2010.

[39] LCPC, "Recommandations pour la prévention des désordres dus à la réaction sulfatique interne," 2007.

[40] B. Lothenbach, G. Le Saout, E. Gallucci, and K. Scrivener, "Influence of limestone on the hydration of portland cements," *Cement and Concrete Research*, vol. 38, no. 6, pp. 848–860, 2008.

[41] M. Al Shamaa, S. Lavaud, L. Divet, J.-B. Colliat, G. Nahas, and J.-M. Torrenti, "Influence of limestone filler and of the size of the aggregates on DEF," *Cement and Concrete Composites*, vol. 71, pp. 175–180, Aug. 2016.

[42] V.-H. Nguyen, N. Leklou, J.-E. Aubert, and P. Mounanga, "The effect of natural pozzolan on delayed ettringite formation of the heat-cured mortars," *Construction and Building Materials*, vol. 48, pp. 479–484, Nov. 2013.

[43] W. Deboucha, N. Leklou, and A. Khelidj, "Blast furnace slag addition effects on delayed ettringite formation in heat-cured mortars," *KSCE Journal of Civil Engineering*, vol. 22, pp. 3484–3490, Sept. 2018.

[44] H. Ranaivomanana and N. Leklou, "Investigation of microstructural and mechanical properties of partially hydrated asbestos-free fiber cement waste (affc) based concretes: Experimental study and predictive modeling," *Construction and Building Materials*, vol. 277, p. 121943, 2021.

[45] G. W. Scherer, "Factors affecting crystallization pressure," in *Internal Sulfate Attack and Delayed Ettringite Formation* (J. S. K. Scrivener, ed.), (Paris), pp. 139–154, Int. RILEM 186-ISA Workshop, PRO 35, RILEM publications, 2004.

[46] L. Divet and R. Randriambololona, "Delayed Ettringite Formation: The Effect of Temperature and Basicity on the Interaction of Sulphate and C-S-H Phase," *Cement and Concrete Research*, vol. 28, no. 3, pp. 357–363, 1998.

[47] J. Crank, *The Mathematics of Diffusion*. Oxford science publications, Brunel University Uxbridge: Clarendon Press, second ed., 1975.

[48] C. L. Page, N. R. Short, and A. El Tarras, "Diffusion of chloride ions in hardened cement pastes," *Cement and Concrete Research*, vol. 11, no. 3, pp. 395 – 406, 1981.

[49] S. W. Yu and C. L. Page, "Diffusion in cementitious materials: 1. Comparative study of chloride and oxygen diffusion in hydrated cement pastes," *Cement and Concrete Research*, vol. 21, no. 4, pp. 581 – 588, 1991.

[50] V. T. Ngala, C. L. Page, L. J. Parrott, and S. W. Yu, "Diffusion in cementitious materials: II, further investigations of chloride and oxygen diffusion in well-cured OPC and OPC/30%PFA pastes," *Cement and Concrete Research*, vol. 25, no. 4, pp. 819 – 826, 1995.

[51] V. T. Ngala and C. L. Page, "Effects of carbonation on pore structure and diffusional properties of hydrated cement pastes," *Cement and Concrete Research*, vol. 27, no. 7, pp. 995 – 1007, 1997.

[52] K. A. MacDonald and D. O. Northwood, "Experimental measurements of chloride ion diffusion rates using a two-compartment diffusion cell: Effects of material and test variables," *Cement and Concrete Research*, vol. 25, no. 7, pp. 1407 – 1416, 1995.

[53] X. Huang, J. Zheng, and X. Zhou, "Simple analytical solution for the chloride diffusivity of cement paste.," *The World of Building Materials*, no. 2, p. 3, 2010.

[54] F. Adenot, *Durabilité du beton : caractérisation et modélisation des processus physiques et chimiques de dégradation du ciment.* PhD thesis, 1992. Thèse de doctorat dirigée par Touray, Jean-Claude Sciences appliquées Orléans 1992.

[55] N. Petrov, *Effets combinés de différents facteurs sur l'expansion des bétons causée par la formation différée d'ettringite.* PhD thesis, Université de Sherbrooke, 2003.

[56] A. Yammine, *Multi-scale modelling and experimental study of damage by internal sulphate attack in cementitious materials : application to ordinary and recycled concrete.* PhD thesis, Nantes University, 2020.

[57] V.-H. Nguyen, N. Leklou, and P. Mounanga, "The effect of metakaolin on internal sulphate attack of the heatcured mortars," *Romanian Journal of Materials*, vol. 49, no. 1, pp. 51–57, 2019.

[58] X. Brunetaud, R. Linder, L. Divet, D. Duragrin, and D. Damidot, "Effect of curing conditions and concrete mix design on the expansion generated by delayed ettringite formation," *Materials and Structures*, vol. 40, pp. 567–578, July 2007.

[59] B. Kchakech, *Étude de l'influence de l'échauffement subi par un béton sur le risque d'expansions associées à la Réaction Sulfatique Interne.* PhD thesis, Universit'e Paris-Est, 2015. Thèse de doctorat dirigée par Toutlemonde, Francois Structures et Matériaux Paris Est 2015.

[60] C. Famy, K. Scrivener, A. Atkinson, and A. Brough, "Influence of the storage conditions on the dimensional changes of heat-cured mortars," *Cement and Concrete Research*, vol. 31, no. 5, pp. 795–803, 2001.

[61] R.-P. Martin, *Analyse sur structures modèles des effets mécaniques de la réaction sulfatique interne du béton.* Theses, Université Paris-Est, Dec. 2010.

[62] B. Bary, N. Leterrier, E. Deville, and P. Le Bescop, "Coupled chemo-transport-mechanical modelling and numerical simulation of external sulfate attack in mortar," *Cement and Concrete Composites*, vol. 49, pp. 70–83, 2014.